Final Report

A PRELIMINARY DESIGN STUDY OF A MICROPARTICLE ACCELERATOR

January 30, 1964 to April 13, 1964

Contract NAS2-1873

Prepared for:

Ames Research Center

National Aeronautics and Space Administration

Moffett Field, California

ION PHYSICS CORPORATION

Burlington, Massachusetts

NOTICE

This report was prepared as an account of Government sponsored work. Neither the United States, nor the National Aeronautics and Space Administration (NASA), nor any person acting on behalf of NASA:

A.) Makes any warranty or representation, expressed or implied, with respect to the accuracy, completeness, or usefulness of the information contained in this report, or that the use of any information, apparatus method, or process disclosed in this report may not infringe privately owned rights; or

B.) Assumes any liabilities with respect to the use of or for damages resulting from the use of any information, apparatus, method or process disclosed in this report.

As used above, "person acting on behalf of NASA" includes any employee or contractor of NASA, or employee of such contractor, to the extent that such employee or contractor of NASA, or employee of such contractor prepares, disseminates, or provides access to, any information pursuant to his employment or contract with NASA, or his employment with such contractor.

Requests for copies of this report should be referred to:

National Aeronautics and Space Administration
Office of Scientific and Technical Information
Washington 25, D. C.
Attention: AFSS-A

FOREWORD

This final report was prepared by those members of the staff of the Particle Physics and Electro-Physics Departments of Ion Physics Corporation involved in "A Design Study for Microparticle Accelerator" under NASA Contract NAS2-1873. The work was administered through the Planetary Science Branch of the Ames Research Center, Moffett Field, California. The technical monitor was James F. Vedder.

Principal contributors to the execution of the study and preparation of this report were:

Dr. K. W. Arnold
R. B. Britton
R. N. Cheever
Dr. A. S. Denholm
Dr. S. V. Nablo
P. R. Wiederhold

ABSTRACT

The preliminary design considerations for a proposed 2 MV microparticle accelerator are discussed. The primary objectives in the study were the attainment of minimum particle path length, very low environmental pressure (~ 10^{-8} torr), accommodation to a possible 10% particle charge loss in flight, and a capability of future extrapolation to higher voltages in a machine having both the particle source and target assembly at ground potential. The design which has evolved is a four-stage device in which the particle is sequentially accelerated into drift tubes at 500 kV negative potential which are then switched to ground while the particle is shielded inside.

A complete description of the accelerator and the method of installation on the proposed site as well as descriptions and specifications of component parts is provided.

TABLE OF CONTENTS

LIST OF ILLUSTRATIONS

1. SURVEY OF POSSIBLE ACCELERATION METHODS

The primary object of this study is to design a machine which can accelerate micron size charged particles to velocities approaching 10^5 meters per second. The particles will have charge-to-mass ratios of 10^1 to perhaps 10^3 coulombs per kilogram. The velocity obtained by releasing a particle in an electric field is:

$$v = \sqrt{\frac{2Vq}{m}}$$

where

v = meters per second, $v << 3 \times 10^8$ m/sec

V = total potential drop - volts

q = coulombs - particle charge

m = kilograms - particle mass

To obtain the 10^5 meters per second, one therefore requires from 5×10^6 to 5×10^9 volts for $\frac{q}{m}$'s of 10^3 to 10^1. Since 10^7 volts is the maximum potential drop available in present-day static field machines, it is necessary to consider all known methods. These are reviewed in the chart.

The potential drop accelerator (method A) as already mentioned is limited to producing final velocities lower than desired or to requiring charge-to-mass ratios on the upper end of those available. It has also the disadvantage that the particle source must be separated from the target by the acceleration potential (millions of volts!). This means that either the source or the target must be inconveniently contained in the pressurized gas environment.

A more versatile acceleration method (B) uses the same constant electric field combined with a variable charge on the particle. With this method, the source and target may both be at ground potential. The positively charged particle may be discharged while in the high voltage negative terminal by passing it through a charge exchange canal (gas cloud) but appreciable negative charging (addition of electrons) would be difficult. Without charge reversal, one is limited to the same 10^7 volt drop available in A. Furthermore, our atomically large particle is multiply charged and the amount of discharging performed within the charge exchange canal would be variable. The result is that one could not accurately predict the final energy of the particle.

Even if we keep our source and target at the same potential and the particle charge invariant, we may still accelerate the particle. In this method (D), the line integral of potential between source and target is zero while a wave in electric potential is propagated through the accelerator. The forward face of this wave (as seen by the particle) is then synchronized with the position of the injected particle and the peak field region is accelerated in phase (theoretically) with the particle position. A similar accelerator (C) uses quantized field regions which are sequentially switched in strength as the particle passes through them. In this latter device, the particle sees an intermittent acceleration rather than the continuous acceleration of the traveling wave.

Choice between the two propagating field methods is determined by the requirement for synchronism. Comparison of our peak particle velocity with that of light $\left(\frac{10^5}{3 \times 10^8}\right)$ shows that we require an electric field which advances either smoothly or intermittently to a maximum of 0.0003 c. This relativistically low velocity is incompatible with the traveling wave method. The lowest wave velocities attained in distributed constant

transmission lines are higher than the highest velocity required in this accelerator. The alternating field accelerator remains, and with this, one can create the required propagation velocity.

Propagating field accelerators may be built in either a linear (open-ended) form or a looped (orbital) form. In choosing between these, we may first say that a linear accelerator using the alternating field principle is capable of accelerating our particle considerably past 10^5 m/sec given the linear space and the money. One can imagine, for instance, a long potential drop-type accelerator tube supported in a pressurized gas vessel. The entire tube is initially raised to a million volts or so negative and this potential falls to ground across a two-foot section at each end. When a particle is injected into this tube, a pressure switch discharging mechanism is triggered serially along the tube to ground (or reverse polarity) of each joint or support as the particle passes through it. The limit is reached when jitter in switching time necessitates long drift spaces and the particle has lost a large percentage of its charge, making further acceleration costs prohibitive.

The looped or orbital accelerator offers the possibility of cyclic acceleration whereby the same acceleration components are used repeatedly instead of once per shot as in the linac. However, a constraining field is now required to make the particle orbit. The field strengths required as as follows:

$$B = \frac{mv}{qr} = \frac{1}{r}\sqrt{\frac{2\,mV}{q}}$$

$$E = \frac{mv^2}{qr} = \frac{2\,V}{r}$$

where:

B = webers/meter^2

v = meters per second

r = orbit radius

V = potential drop previously suffered by particle

E = volts/meter

Let:

$\frac{q}{m} = 10^2$, then $\frac{m}{q} = 10^{-2}$

$v = 10^5$ meters per second

$r = 3$ meters

Then:

$$B = \frac{10^{-2} \cdot 10^5}{3} = 3.3 \times 10^2 \text{ webers/meter}^2 = 3.3 \times 10^6 \text{ gauss}$$

$$E = \frac{10^{-2} \cdot 10^{10}}{3} = 3.3 \times 10^7 \text{ volts/meter}$$

It is clear from this calculation that magnetic constraint of these particles is out of the question since magnetic forces are a function of velocity. However, electric constraint to an orbit is possible. Fields in excess of this value may be held over a gap of one centimeter. Various problems include: holding this field over the area of a 20 meter long particle trajectory, programming the field to match the square of the particle velocity, and the design of a field curvature to create stable orbits.

In view of the difficult design associated with the electrically constrained orbital accelerator, it is felt that the linear accelerator using alternating fields is the best solution.

Since higher voltage gradients can be maintained across short vacuum gaps than along potential drop-type accelerator tubes, the minimum length accelerator consists of drift tubes separated by vacuum gaps. These tubes are initially all at high negative potential and are switched to ground serially when the microparticle is shielded within. This approach is also necessary if pressures of $\sim 10^{-8}$ torr are to be reached, due to the limited conductance and significant outgassing of an extended acceleration tube of conventional (graded) geometry. It is necessary in a vacuum insulated machine to provide a high voltage feedthrough bushing both to support the drift tubes off the grounded walls of the vacuum vessel and to bring the high voltage power to the tubes through the vessel wall. From the standpoints of safety and reliable performance, the high voltage power is best generated and distributed in a high pressure inert gas environment, so that the bushing should be of the type that operates from pressurized gas into vacuum. Also, the environment necessary for operation of the so-called pressure, or triggered arc, switch is thus provided. This is the only type of switch known to be capable of switching very high voltages in very short times. Basically, it consists of a spark gap which holds off the high voltage until a smaller gap at either end is broken down by a lower voltage switching pulse. The small discharge then initiates a high current arc or breakdown in the main gap.

2. SYSTEM DESIGN OF PROPOSED ACCELERATOR

2.1 SEQUENCING

There are two approaches to the sequencing of a pulsed accelerator. The pulsing can be accomplished on signals obtained either from particle detectors at each stage or from a program generator actuated by a single detector at the outset of the machine and made variable to accommodate the charge-to-mass ratio range. A programmed machine would have to have increased drift tube lengths to allow for a possible 10% charge uncertainty over the entire length of the acceleration path from the detector on. On the other hand, the lengths required for particle detectors, either optical or electrical, result in an approximately equal increase in accelerator length for a 2 MV machine. The stagewise detection approach offers the ultimate in accommodation of particle charge uncertainties but only at the expense of great electronic complexity and reduced reliability. This has seemed too great a price to pay for the increased flexibility and so the programmed sequencing technique has been adopted for the proposed accelerator.

2.2 STAGING

Since shortness of the acceleration path is an overriding consideration in the accelerator design, the stage voltage (hence, number of stages) should be chosen so as to minimize the path length. Each stage consists of an acceleration gap followed by a drift tube. The gap need only be long enough to safely hold the stage voltage between adjacent drift tubes. It is known from experiments conducted at IPC and elsewhere that the (vacuum) gap required for insulation of a voltage V between similar electrodes is proportional to V^2 for sufficiently large gaps (over 1 cm in the present case). The most pertinent current data show the constant of proportionality to be about 5 cm/MV^2.

The drift tubes are sufficiently long to shield the microparticles from fringing electric fields and, moreover, to provide such shielding over a distance long enough to cover uncertainties in the particle position and in the time at which the tube is switched to ground. In any cross section of a drift tube, the maximum deviation from tube potential occurs at the axial point. It is easily shown that the axial potential deviation is given approximately by

$$\Delta V \, e^{-(b_1 z/r)}$$

where ΔV is the axial potential deviation in the end plane of the tube, z is distance from the end plane (taken as positive), r is the tube radius, and $b_1 = 2.405$ is the first zero of the Bessel function of the first kind, zeroth order. Thus, if shielding is required to one part in a thousand, the corresponding value of z is about three tube radii and the total shielding length for a drift tube is twice this or three diameters. Shielding to one part in a thousand is required in order to minimize the energy differences associated with particle position uncertainties. These energy differences lead to amplification of position uncertainties in succeeding stages of the accelerator thus necessitating an undesirable increase in drift tube length.

The length of drift tube required to accommodate uncertainties and errors (the error length) increases somewhat more than linearly with particle speed. This is because some errors may be expressed as a time interval which is the same for each stage (length linear with velocity) while others are cumulative. The average error length required is chiefly determined by the total accelerator voltage and the magnitudes of the errors and

uncertainties and depends only weakly on the number of stages into which the accelerator is divided. Thus, denoting the average error length by ℓ (cm), the stage voltage by V(MV), and the total accelerator voltage by V_T (MV), the total accelerator length, L (cm), can be written as

$$L = \frac{V_T}{V} (5 V^2 + 6r + \ell)$$

Ignoring for the moment the slight variation of ℓ with V and setting the derivative of L with respect to V equal to zero, the value of stage voltage, V_m, giving minimum accelerator length can be found to be

$$V_m = \sqrt{(6r + \ell)/5}$$

In order to obtain maximum particle transmission, as discussed later in Subsection 3.5.1, the drift tube inside diameter has been taken to be 2.5 cm. Thus, even for zero error length, the optimum stage voltage is about 1.2 MV, which is well in excess of bushing capabilities. The design stage voltage of 0.5 MV (four stages) is the closest possible approach to the optimum voltage in the present state of bushing technology.

2.3 POWER SUPPLY

2.3.1 Present Requirements

High voltage power may be supplied to the accelerator either by distribution from a single supply or by providing each stage with a separate supply. Van de Graaff, ICT, or even conventional transformer-rectifier power supplies could be used with the distribution system. In the case of separate supplies, however, only the Van de Graaff type can be made sufficiently small to be practical. Cost wise, there is little to choose between these two approaches. The reduction in reliability due to somewhat increased complexity in the case of separate supplies can be offset by a preventive maintenance program on the generators. Since these devices can be ruggedly built for long trouble-free service, the preventive maintenance program necessary to ensure a tolerable level of lost accelerator time is not onerous. If a spare generator is provided, the program can be carried out by rotation thus reducing lost time to a negligible level.

In the case of a single supply, the stages would have to be connected to the high voltage linethrough high impedance isolation resistors to prevent the discharge of all succeeding stages when any given stage is pulsed. However, it does not appear feasible to reduce the capacitance associated with these resistors much below 10 pf which is about one-tenth of the bushing capacitance. This shunt capacitance constitutes an rf connection between stages which results in voltage degradation of all succeeding stages when a given stage is pulsed. The degradation is cumulative, the first stage being totally unaffected and the last stage most affected. Because of the large ratio of shunt capacitance to bushing capacitance, the voltage sag may be as large as 10% for the last stage. There is also the additional possibility that the large amounts of rf energy transferred among the stages during pulsing of a given stage may interfere in other ways with succeeding stages, perhaps causing premature grounding. On the other hand, the separate supply

approach provides almost total isolation of the stages. There still remains a connection between adjacent stages due to the capacitance between drift tubes, but this will be, or can be made, very small indeed. Furthermore, any small stage voltage sagging which may occur can be compensated by programming the voltage sequence, which is not possible in the case of a single supply. Multiple supplies also eliminate the clutter involved in a high voltage distribution system. Thus, this approach has been chosen for the proposed microparticle accelerator chiefly because of the increased flexibility and stage isolation it provides at no increase in cost and little increase in preventive maintenance requirements.

2.3.2 Extension Possibilities

When and if the accelerator is extended by the addition of stages, it may be possible, provided operational experience and additional experiments indicate feasibility, to introduce a limited high voltage distribution system wherein each small Van de Graaff generator supplies its own and the two adjacent stages. The original four generators might eventually, then, supply a twelve-stage machine which would occupy very nearly the full vertical space available for the microparticle accelerator. The generators will be designed to provide sufficient current to enable this modification.

It may also prove possible in the future to modify the accelerator so as to use the bushings at both positive and negative potential, thus doubling the effective stage voltage. This suggestion is based on the idea of replacing the damping resistor in the bushing discharge circuit with an appropriate inductance to create a high "Q" resonant circuit. If, then, the triggered arc switch would or could be shut off after one half cycle of oscillation, the bushing would hold at a voltage of + 0.5 MV so that the microparticle would then be accelerated through 1 MV in the following gap instead of 0.5 MV. The arrangement of high voltage components in the accelerator has been so conceived as to facilitate this modification should future research warrant it.

It might be mentioned here that yet another possibility for expansion of accelerator capability is the future development of bushings with increased voltage capacity. In this connection, the Van de Graaff power supplies will be designed for 0.75 MV although the present specification is for 0.5 MV.

2.4 DESCRIPTION OF ACCELERATOR

Two cut-a-way views of the proposed machine are given in Figs. 1 and 2. There are four 500 kV stages, each stage being supplied (separately) by a small Van de Graaff generator (8)* through a pressure-to-vacuum graded high voltage bushing (7). Drift tubes (5) are supported from the bushings and each such assembly is pulsed from negative polarity to ground when the microparticle is in the proper position within the tube. The pulsing is accomplished by firing the triggered arc switch (10) which discharges the bushing through the damping resistor (9). This resistor dissipates the energy stored in the bushing, thus preventing oscillations which could result in considerable rf noise radiation.

The microparticles enter the accelerator through a three-element lens, of which the first element is a tube contained in the source assembly (1), the second element is the gate valve (2) itself, and the third element a tube (4) mounted in the wall of the main vacuum vessel (20). This last tube is at a potential of -5 kV. The focusing of the lens is varied by adjusting the potential of the first electrode. The drift tube lengths are such that a 10% charge loss can be tolerated from the beginning of the accelerator so that the machine may be preprogrammed for each charge-to-mass ratio. Thus, only one particle detector is required at the beginning of the acceleration sequence. This is contained within the final lens element (4) in the form of a shielded ring capacitor. In order to minimize input capacitance, the detector preamplifier and amplifier (3) are placed very close to the detector and are also at a potential of -5 kV.

*All parenthesized numbers in Subsection 2.4 refer to Figs. 1 and 2.

The total length of the acceleration path (from the source to the shielded position within the last drift tube) is about 125 cm. The overall length of the machine (from the source side of the entrance gate valve to the target side of the exit gate valve) is about 190 cm. The inside diameter of the cylindrical main vacuum vessel is 4 ft with the bushings arranged in diametrically opposed tandem pairs. The pressure vessels (6) surrounding each bushing outside the main vacuum vessel are a little over 2 ft long so that the overall diameter of the accelerator is about 8.75 ft. The drift tube lengths, bushing spacings, etc., have all been designed so that, at some later date, the bushings may be used at both positive and negative 500 kV thus doubling the acceleration voltage. Further research will be required before this becomes possible, however, and in the meantime, the extra lengths and spaces provide a safety margin which may prove useful until the operational characteristics of the machine have been fully explored.

To provide access to its interior, the main vacuum vessel is flanged at the bottom. In order to realize this access, the vessel must be hoisted up off the supporting stanchions (17). This seemingly awkward placement of the flange at the bottom rather than the top of the vessel is necessary because this same flange is the mounting surface for any additional stages which may be added to the accelerator in the future to increase its capacity. Addition of such stages would require enlargement of the hole in the second floor (19) and probably the addition of structural steel beneath the stanchions, either in the form of horizontal beams connecting to the existing second floor joistwork, or vertical beams extending downward to pads at the first floor level.

Leveling of the accelerator is accomplished by adjustment of the leveling bolts (22) which support the machine off the stanchions (17). Two 12-inch viewing ports (11) have been provided in the main vacuum vessel and two ultra-high-vacuum, 6-inch diameter, stainless steel gate valves (2)

in order that the vessel need not be let up to atmosphere while servicing the source and target assemblies. The main vacuum vessel is pumped by a 9-inch mercury diffusion pump (12) backed by a smaller mercury booster diffusion pump, a trap, and a water lubricated forepump. Ahead of the 9-inch pump is a freon cooled baffle (13) which is connected to the top of the main vessel via a 12-inch diameter elbow. The presence of a cryopumping* panel in the main vacuum vessel obviates the necessity for the usual liquid nitrogen trap ahead of the freon baffle. This cryopumping panel consists of two heat shields (14) and a liquid nitrogen filled buffer (15) enclosing a liquid helium filled panel (16). Pumping is accomplished via louvres in the nitrogen panel. Covering the cryopumping panel and the walls of the main vacuum vessel is a steel grid (21) biased to several kilovolts positive potential. This grid serves to electrically isolate the panel and vessel walls from the bushings and drift tubes and its presence is considered necessary for the bushings to maintain full rated voltage. The use of mercury diffusion pumps and a water lubricated forepump is also dictated by bushing behavior since there is evidence that the presence of even small amounts of oil in the bushing environment may cause degradation of its voltage performance.

Floor plans for the second floor accelerator installation and for a mezzanine level above the second floor supporting microparticle source ancillary equipment are shown in Figs. 3 and 4 and an artists rendering of the accelerator area is provided in Fig. 5. Fig. 6 shows how the various electronic and electrical components fit together and Fig. 7 similarly illustrates the vacuum and pressurization systems.

*Cryogenic (condensation) pumping.

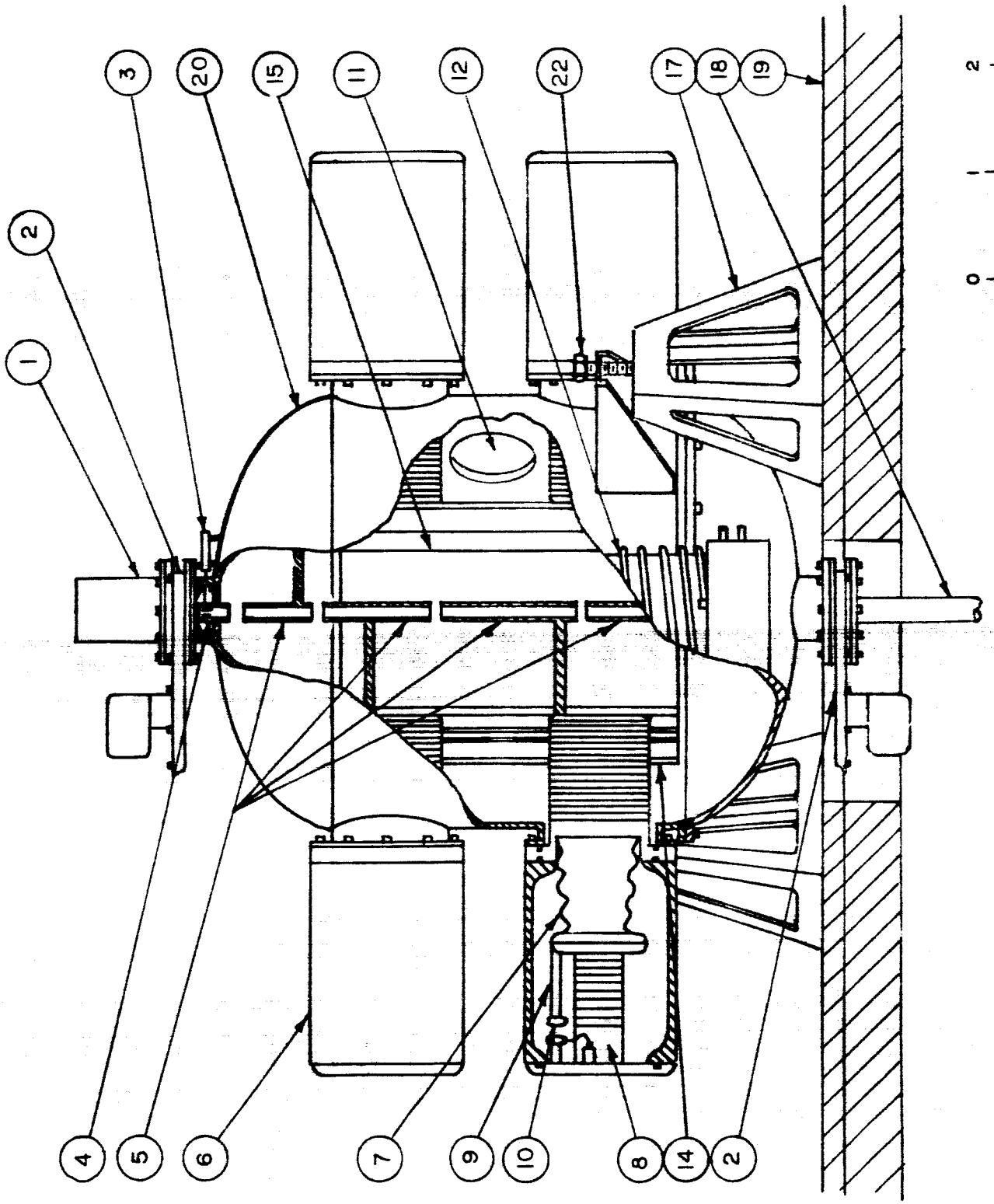

FIG. 1-SIDE VIEW OF ACCELERATOR

1-615

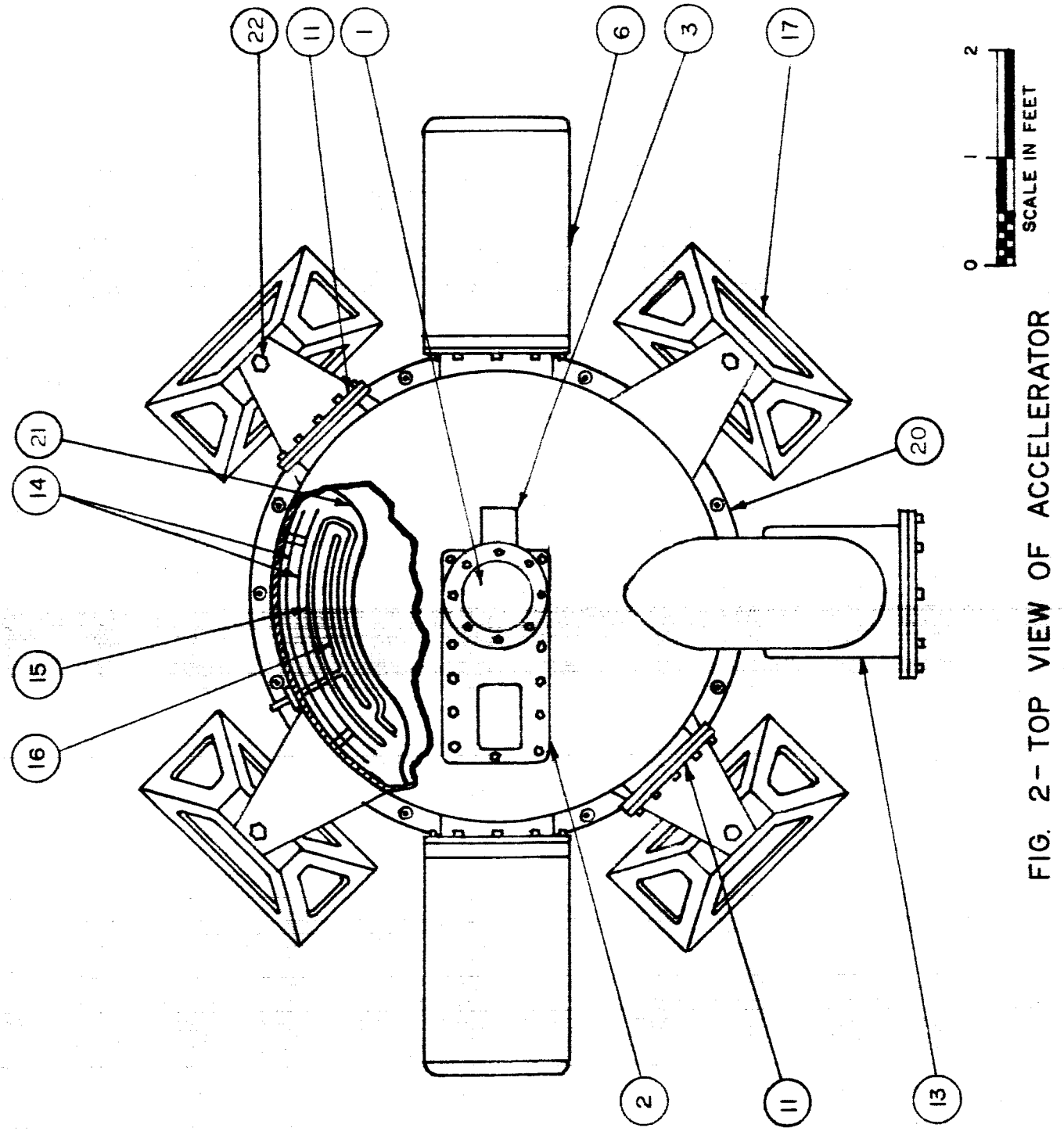

FIG. 2- TOP VIEW OF ACCELERATOR

1-616

Key to Figures 1 and 2

(1) microparticle source

(2) ultra-high-vacuum 6-inch diameter gate valve

(3) detector preamplifier-amplifier

(4) final lens element containing detector

(5) drift tubes

(6) pressure vessel

(7) pressure-to-vacuum graded high voltage bushing

(8) Van de Graaff generator

(9) damping resistor

(10) triggered arc switch

(11) viewing port

(12) 9-inch mercury diffusion pump

(13) freon cooled baffle

(14) heat shields

(15) liquid nitrogen panel

(16) liquid helium panel

(17) supporting stanchion

(18) tube into target chamber

(19) second floor of building

(20) main vacuum vessel

(21) biased steel mesh liner (not shown in Fig. 1)

(22) leveling bolt

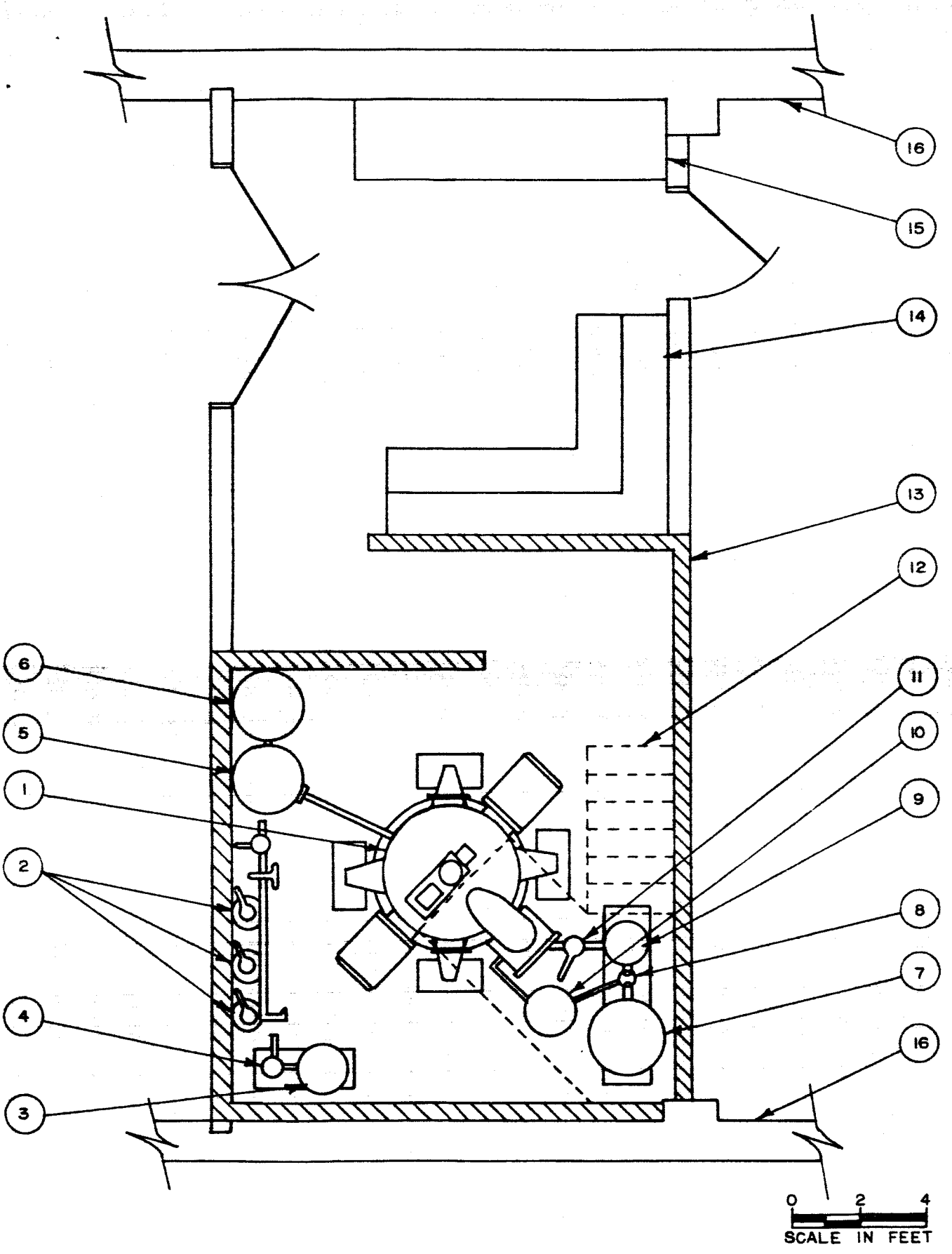

FIG. 3-PLAN VIEW OF SECOND FLOOR SHOWING MICROPARTICLE ACCELERATOR AND ANCILLARY EQUIPMENT

1-643

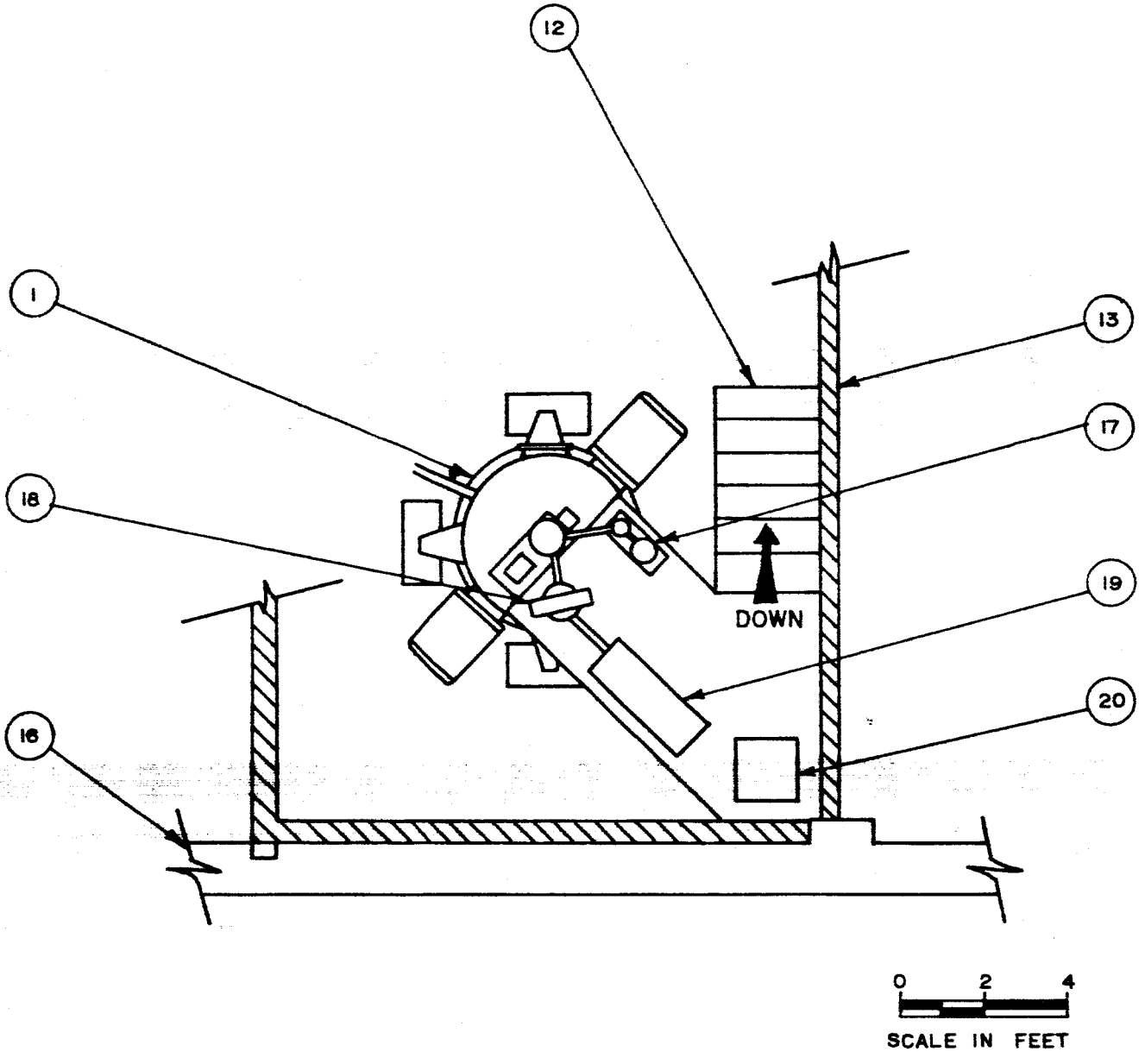

FIG. 4 - PLAN VIEW OF SECOND FLOOR MEZZANINE SHOWING MICROPARTICLE SOURCE ANCILLARY EQUIPMENT

I-644

Key to Figures 3 and 4

(1) microparticle accelerator as illustrated in Figs. 1 and 2

(2) gas storage cylinders (CO_2, N_2, SF_6), valving and gauges

(3) roughing pump for evacuating pressure vessels before pressurization

(4) cold trap

(5) liquid helium dewar

(6) liquid nitrogen dewar

(7) water lubricated forepump

(8) mercury-water condensing trap (freon cooled)

(9) booster pump (2-inch mercury diffusion type)

(10) freon refrigeration units (2)

(11) 2-inch right angle high vacuum valve

(12) stairs to mezzanine (stairs and mezzanine shown dashed on second floor plan)

(13) radiation shielding wall

(14) control console and electronics

(15) work bench

(16) outside wall

(17) microparticle source pumping system

(18) charging beam analyzing magnet

(19) charging beam ion source assembly

(20) magnet and source power supplies

FIG. 5 ARTIST'S RENDERING OF MICROPARTICLE ACCELERATOR INSTALLATION

I-648

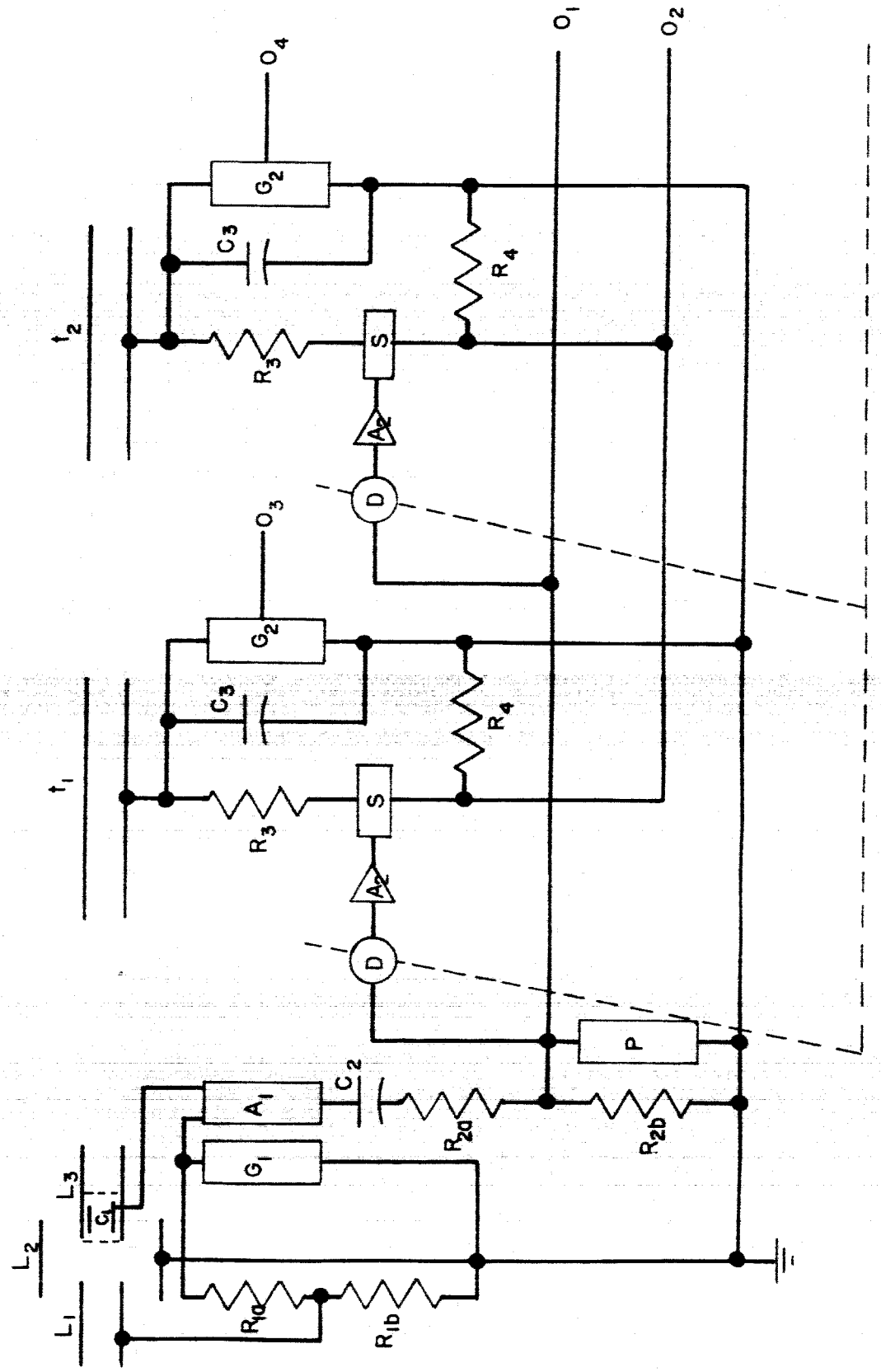

FIG. 6 - ELECTRONIC BLOCK DIAGRAM (FINAL TWO STAGES OMITTED)

Key to Figure 6

L_1, L_2, L_3	-	focusing lens elements
C_1	-	detector capacitance
R_{1a}, R_{1b}	-	voltage divider for obtaining focusing voltage
G_1	-	preacceleration voltage supply
A_1	-	detector preamplifier-amplifier
C_2	-	blocking capacitor
R_{2a}, R_{2b}	-	voltage divider for signal attenuation
P	-	detector pulse simulator
D	-	variable delay module
A_2	-	pulse amplifier
S	-	triggered arc switch
R_3	-	damping resistor
R_4	-	pulse monitoring resistor
t_1, t_2	-	drift tubes
C_3	-	bushing plus Van de Graaff generator capacitance to ground
G_2	-	Van de Graaff generator
O_3, O_4	-	high voltage monitoring outputs
O_2	-	oscilloscope signal output for viewing bushing firing sequence
O_1	-	oscilloscope trigger output for phasing with bushing firing sequence

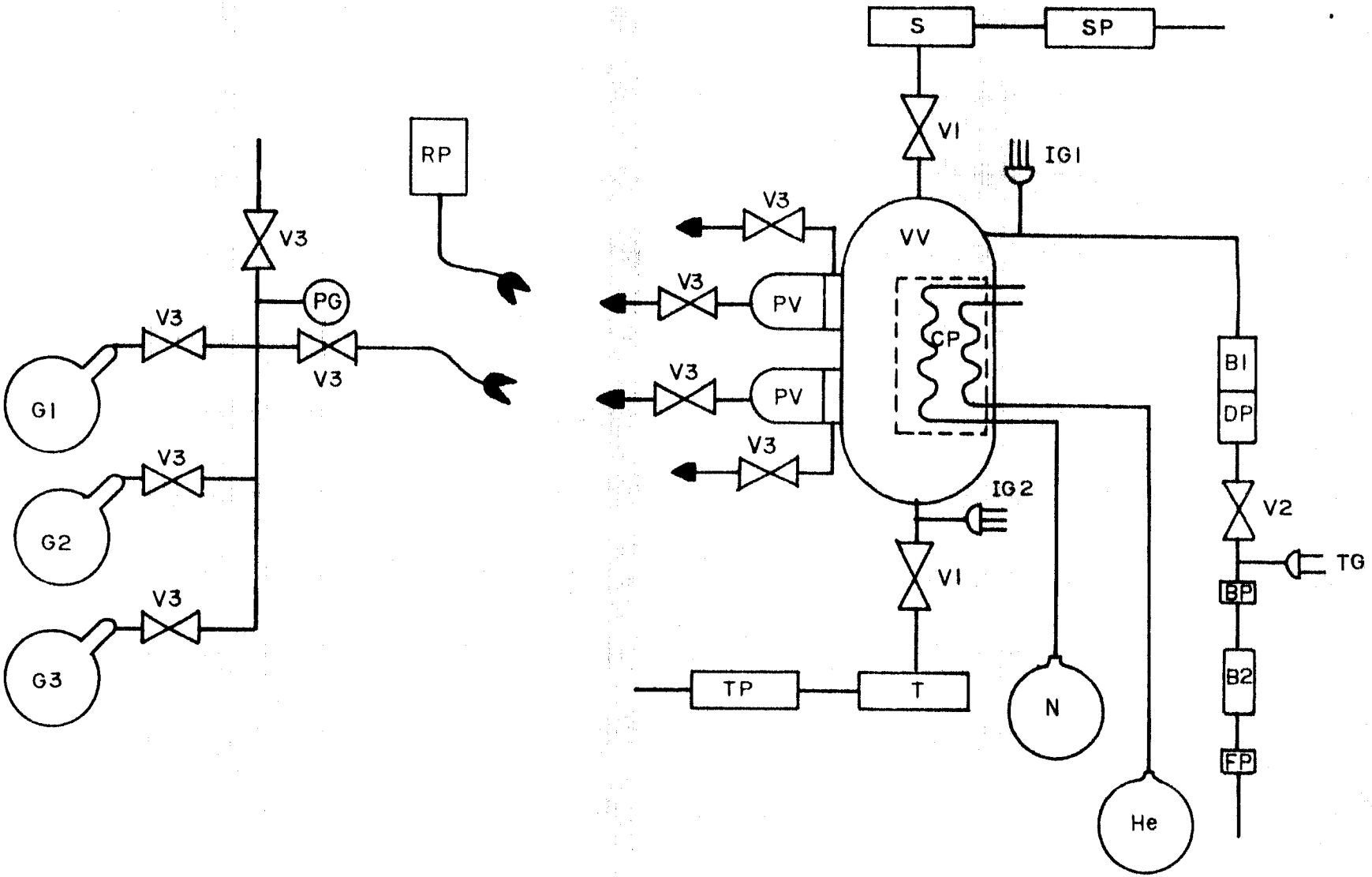

FIG. 7 - VACUUM AND PRESSURIZATION SYSTEMS BLOCK DIAGRAM
(TWO PRESSURE VESSELS OMITTED FOR CLARITY)

Key to Figure 7

FP	forepump
B2	freon cooled trap
BP	Booster diffusion pump
TG	thermocouple type vacuum gauge
V2	high vacuum right angle valve
DP	main diffusion pump
B1	freon cooled baffle
IG1, IG2	ionization type vacuum gauges
N	liquid nitrogen dewar
He	liquid helium dewar
CP	cryogenic (condensation) pump panels
V1	ultra high vacuum gate valve
VV	main vacuum vessel
PV	pressure vessel
V3	standard high pressure gas valve
PG	pressure gauge
G1	carbon dioxide gas reservoir
G2	nitrogen gas reservoir
G3	sulphur hexafluoride gas reservoir
RP	roughing pump
S	microparticle source assembly*
SP	source pumping system*
T	target assembly*
TP	target pumping system*

* These items are not delineated in the specifications since they are to be supplied by NASA-ARC.

3. DESIGN OF SUBSYSTEMS FOR PROPOSED ACCELERATOR

3.1 DELINEATION OF MAJOR SYSTEMS AND SUBSYSTEMS

It is convenient to think of the accelerator as being comprised of two major systems, the primary or accelerating system and the secondary system or envelope. The accelerating system can be subdivided into five major subsystems as follows:

1. Van de Graaff generator;
2. triggered arc switch and damping resistor;
3. pressure to vacuum graded high voltage bushing and steel mesh tank liner;
4. detection, sequencing, and arc switch initiation electronics; and
5. lens, detector, pre-acceleration supply, and drift tubes (acceleration path).

The envelope can be subdivided into the four major subsystems following:

1. tankage and supporting structures;
2. vacuum equipment;
3. pressurization equipment; and
4. radiation shielding.

3.2 ACCELERATING SYSTEM DESIGN

3.2.1 Generator

The Van de Graaff type electrostatic generators (G_2)* will operate in an inert gas atmosphere (N_2, CO_2) at a pressure not to exceed 300 psi

*All parenthesized symbols in Subsection 3.2 refer to Fig. 6.

while generating at least 50 μa at a potential magnitude of at least 500 kV, negative polarity. The voltage setting mechanism and the regulation will be such that the total uncertainty in the terminal voltage will be no more than ±5% at 500 kV. The maximum diameter of the generators will not exceed 10 in. and the overall length will not exceed 18.5 in. including the mounting flange, which also serves to seal the pressure vessel ((6) Figs. 1 and 2). The generators will provide low voltage output signals (O_3, O_4) proportional to their terminal voltages to enable high voltage monitoring with a d. c. microammeter. The generators will be built for heavy duty to provide long, maintenance-free periods of operation. The voltage and current ratings specified for the generator are all that is necessary for the present application, but the actual design goals will be 200 μa at 750 kV to provide for future expansion. These and the size and regulation specifications have been based on what is thought to be achievable in the present state of generator technology.

3.2.2 Switch

The damping resistor (R_3) will be so chosen that the circuit consisting of the bushing-generator capacitance (C_3) and the residual inductance in the discharge path (not shown) will be at least critically damped to minimize rf radiation. In addition, it must satisfy the joint condition with the arc switch (S) that the total of switch delay time (the time from full off to full on) plus capacitance discharge time (the time required for the voltage to decay to 0.1% of the initial voltage) shall not exceed 1 μsec. The triggered arc switch will stand off at least 500 kV at less than 300 psi of inert gas insulation and be capable of being actuated with a 50 kV pulse. The pulse monitoring resistor (R_4) will be less than 0.001 of the value of R_3. Its purpose is to provide a signal during stage discharge on the output line (O_2) so that the stage "firing" sequence may be viewed on an external oscilloscope (not shown). The switch delay plus capacitance discharge time

specification of 0.1 μsec is thought to be conservative in view of the present state of switch development.[1, 2, 3, 4] Recent work at IPC with a 160 kV switch has demonstrated delay times of less than 0.1 μsec and a capacitance discharge time of 0.4 μsec seems quite reasonable.

3.2.3 Bushing

The high voltage pressure-to-vacuum graded bushing (included in capacitance C_3) will be capable of carrying a potential of magnitude at least 500 kV, negative polarity, into the main vacuum vessel. It will be designed to work with an internal pressure of no more than 300 psi of sulphur hexafluoride (SF_6) and in an external pressurized environment of no more than 300 psi of inert gases (N_2, CO_2). It will not exceed 10 in. diameter nor shall it be longer than 23 in. overall, including mounting flange, which forms the pressure-to-vacuum seal. The isolation grid to screen the bushings from the inside wall of the main vacuum vessel will be made of 304 stainless steel wire with a mesh spacing small compared to the grid-wall separation distance. The grid will be at least 80% transparent. The specification of 304 stainless steel made here and elsewhere in the report is based on the apparently superior voltage breakdown characteristics of this material (as compared to other more easily fabricated stainless steels). The specifications of bushing size and performance are consistent with the current technology.[5]

3.2.4 Electronics

The detector preamplifier-amplifier (A_1) will provide an output pulse of at least 50 V amplitude over the entire charge-to-mass ratio range of 20 to 500 coul/kg with the chosen detector element. The rise (and fall) time of the output pulse will be no more than 10% of the total pulse length. The blocking capacitor (C_2) serves to couple the detector signal to ground

potential and in the process adds ± 5 V ripple and/or noise since the pre-acceleration supply is regulated to ± 0.1% (see Subsection 3.2.5). The 50 V amplitude output of the detector preamp-amp ensures a signal-to-noise ratio of 10:1. The resistors R_{2a}, R_{2b} form a potential divider and should satisfy $R_{2a}:R_{2b} = 4:1$. The output of this divider consists of 10 V of signal and 1 V of "noise".

The variable delay module (D) will have a range of at least 10-1000 μsec. This may be subdivided into decades of 10-100, 100-1000 μsec. The accuracy of delay will be at least ± 0.2% of full scale on both ranges. The delay modules will require an input trigger signal of at least 5 V so that activation cannot be effected by the 1 V "noise", and shall be variable in two modes. In the first of these, individual modules will be set separately one relative to another in a sequence of ratios. In the second, a ganged control of all four modules simultaneously will set the absolute time scale corresponding to the particular charge-to-mass ratio being accelerated. These specifications of delay module performance have been chosen in accordance with those of commercially available equipment.

The pulse amplifier (A_2) must amplify the output of the delay module so as to produce a pulse of at least 50 kV amplitude with a rise time (to 50 kV) of no more than 0.9 μsec. This pulse, in turn, will trigger the arc switch. Amplifiers of this, or very similar, kind are sold commercially.

The detector pulse simulator (P) will provide a signal output similar in all important respects to that of the detector preamplifier-amplifier as attenuated in the potential divider. This output will be produced on command of the accelerator operator and is to be used for system checkout. An output (O_1) will be provided so that the detector or detector simulator signal may be used to trigger an external oscilloscope for viewing the pulsing sequence on output O_2.

3.2.5 Acceleration Path

Acceleration Path Elements

The focusing lens will consist of three elements (L_1, L_2, L_3). The first of these will consist of a stainless steel tube of 2.5 cm i.d. and appropriate length mounted within the microparticle source. The final element will be fashioned of 304 stainless steel tube 6.5 cm in length and 2.5 cm i.d. It will be mounted in the entrance port opening in the end wall of the main vacuum vessel on a suitable insulator and will protrude 2.5 cm beyond the inner surface of the vessel wall. The middle element will consist of the gate valve walls. Tubes L_1 and L_3 must be separated by a distance which is sufficient to provide clearance for the workings of the gate valve (approximately 2 inches). The final tube will be held at a potential of -5 kV ±0.1% by the preacceleration voltage supply (G_1). The potential divider R_{1a}, R_{1b} will be so constructed as not to prove an excessive current drain on the supply G_1 and to provide the proper focusing voltage to the first tube, as determined from experiments. The first 2.5 cm of the final tube will be screened off by two 98% transparent conducting grids to form a detector chamber within which will be placed a suitable capacitive probe to detect the transits of charged microparticles. Suspended from the four bushings will be four drift tubes (t_1, t_2, etc.) fashioned of 304 stainless steel tube having an i.d. of 2.5 cm. The gap between L_3 and t_1 will be 2.5 cm but the gaps between all other tubes will be 5 cm. The sequence of drift tube lengths will be 18.0 cm, 29.3 cm, 40.6 cm, and 52.8 cm. The distance from the end of the final tube to the inside surface of the end wall of the main vacuum vessel will be 5.3 cm, measured on axis. The axial positions of the drift tubes must be maintained to within ±0.25 cm. Concentricity of the tubes with the axis of the main vacuum vessel must likewise be ±0.25 cm. These tolerances are considered reasonable in view of those ordinarily achieved in the construction of much larger accelerators

of similar complexity. The gaps between tubes have been chosen long enough to insulate 1 MV (as would be necessary with the doubling scheme outlined in Subsection 2.3) in the light of the best data available. The end gaps need only insulate one-half this voltage. However, they must be larger than the 1.25 cm indicated by the dependence of gap length on the square of gap voltage because of the effects of the nearness of the large area of the end plates of the main vacuum vessel. Here again, the gap length specified is consistent with the best data available.

Radial Focusing

The i.d. of 2.5 cm which has been specified for acceleration path elements was originally chosen on the basis of approximate calculations of particle trajectories which indicated that this dimension should be adequate. These calculations neglected the fringing electric fields in the acceleration gaps (which produce focusing) and assumed particle energy changes occurred in discrete increments at the ends of the gaps. Computer calculations of actual particle trajectories (rays) through the accelerator have since been made in order to determine what range of input conditions (radial position and direction of travel) is allowable. The entrance conditions for which the calculations have been made correspond to the numbered positions in the diagram of Fig. 8. The ordinate here is the angle between the direction of particle travel and the axis of the accelerator while the abcissa is the radial position. Because of the cylindrical symmetry, no calculations are necessary in the lower two quadrants of the diagram. The total range of radial position encompasses a diameter of 1/16 in. corresponding to the fact that it is known that all particles from the ARC source can be put through a hole of this diameter, a distance of 5 in. from the source at extraction voltages lower than 5 kV. The positions and travel angles of particles corresponding to the numbered points at a target 1 m from the end of the accelerator are shown in Figs. 9 and 10 for 2 MV and 4 MV total potential drop. At 4 MV,

all calculated rays fall within a circle of diameter 0.3 cm at the target while at 2 MV several extreme rays impinge on the drift tubes and the radial scatter at the target is much more severe.

It is apparent that only particles entering within a small diameter and at very small angles of travel end up at the target within the hoped-for 1 cm diameter spot at the lower energy. This results from overfocusing in the first acceleration gap, which proves to be a very short focal length lens. The focusing action is illustrated in Figs. 11 and 12 which show some typical rays through the accelerator at both energies. The zero axial position for these calculations has been taken 1 cm from the detector on the source side for convenience in calculating since the choice allowed advantage to be taken of a symmetry. The travel angles are so small that there would be virtually no difference in the calculations had the starting position been taken at the beginning or end of the detector. The plotted points have been joined by straight line segments for the sake of simplicity, although the actual particle trajectories are of course smooth curves. All rays are focused so as to cross the axis of the accelerator at about 8.75 cm which is the center of the first acceleration gap. In the range from 0 to 8.75 cm, the particle motions are very abrupt; however, the computer output was taken at intervals too coarse to show this detail (although the calculations themselves were performed over very fine intervals). Accordingly, trajectory segments in this range have simply been omitted. It is clear that, in the 4 MV case, the lens action of the succeeding acceleration gaps tends to compensate the overfocusing of the first gap so as to bring all particles into close proximity at the target. This is not true in the 2 MV case because of the weaker focusing action of all gaps but the first. If it should be thought necessary in the future, the first acceleration gap could be made a much weaker lens by the use of shielding grids to reshape the electric field.

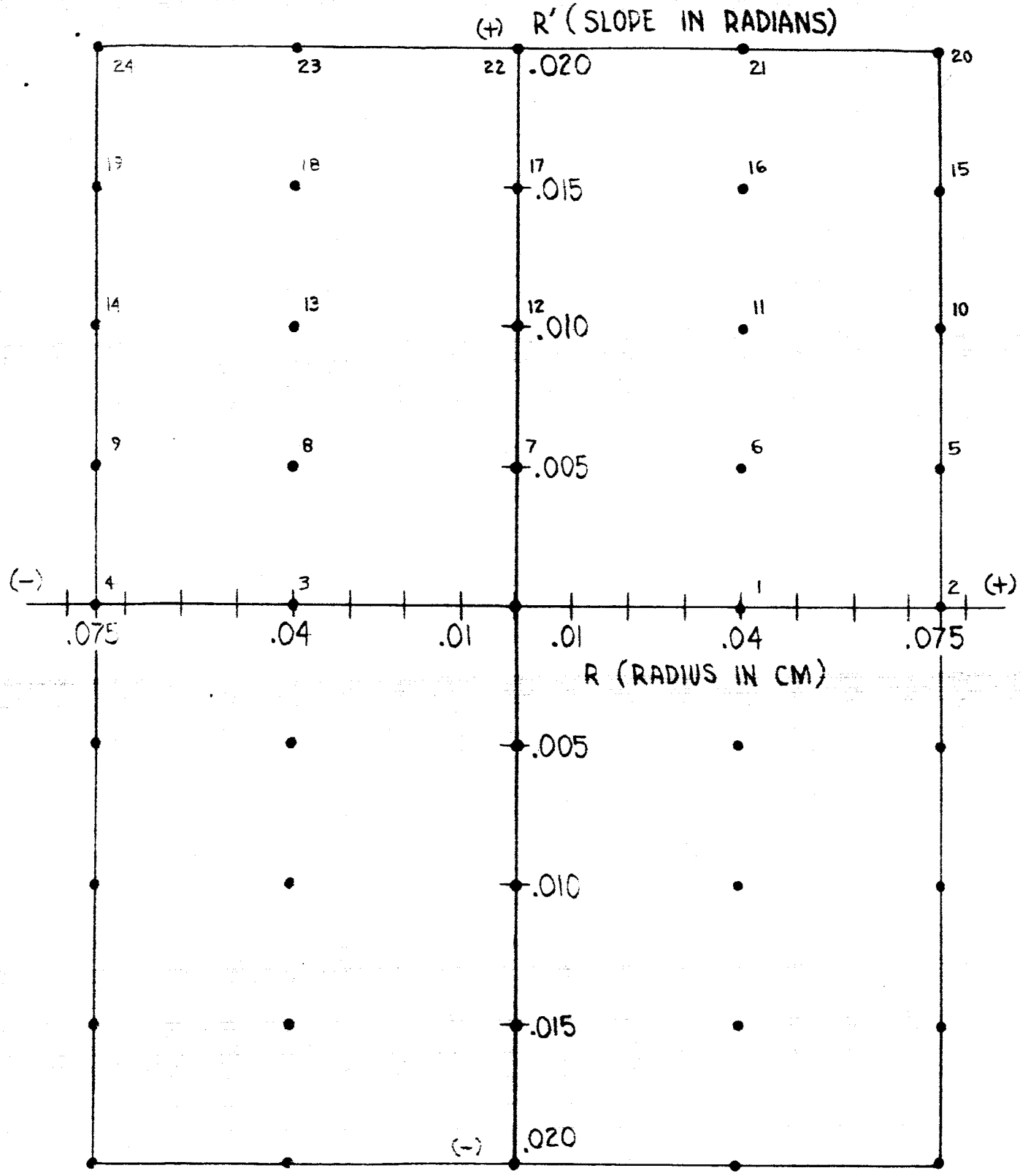

FIG. 8 - EMITTANCE AT DETECTOR USED AS INPUT FOR FORWARD RAY TRACING

1-645

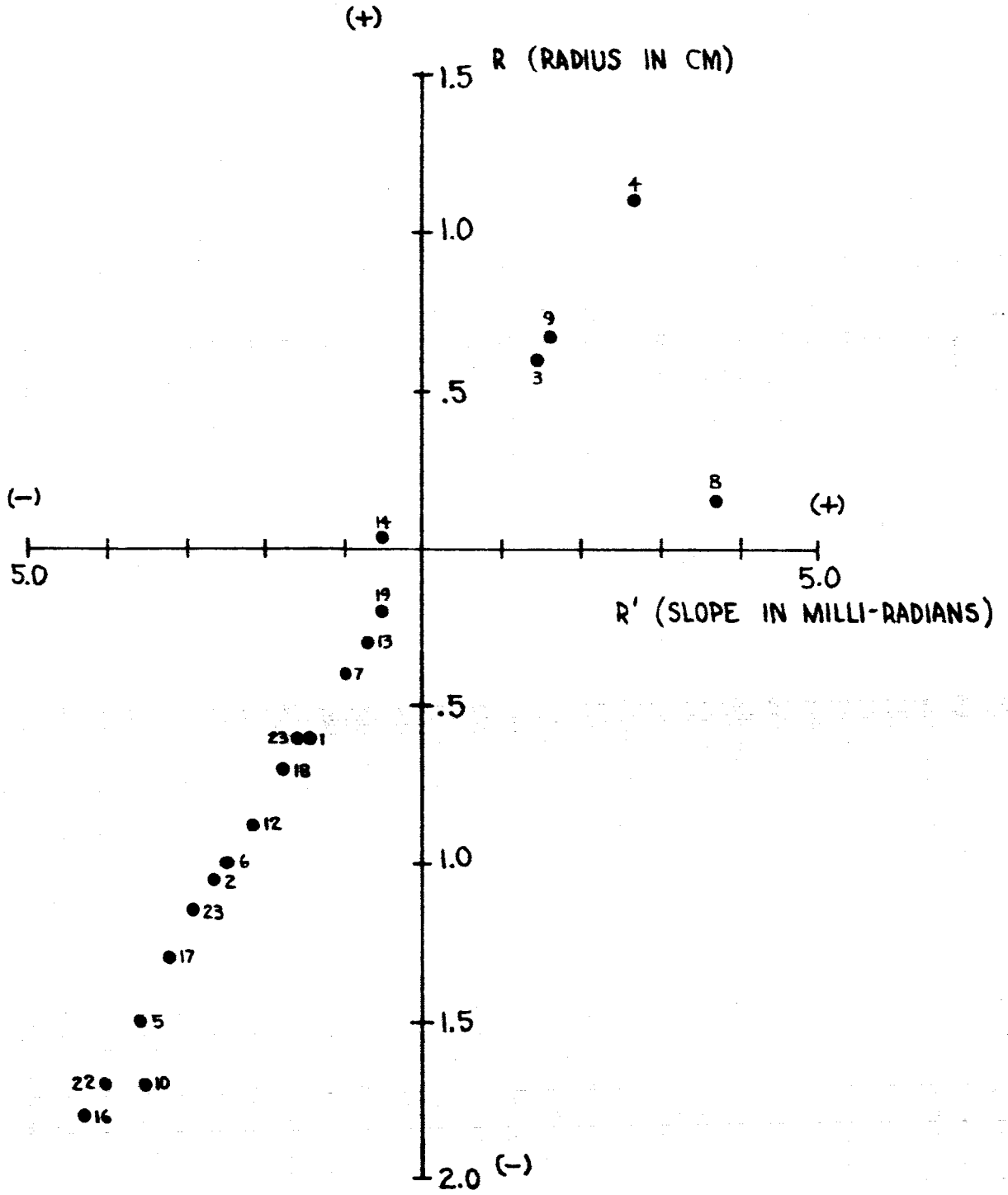

FIG. 9 - INPUT EMITTANCE PROJECTED TO TARGET (2 MV)

1-646

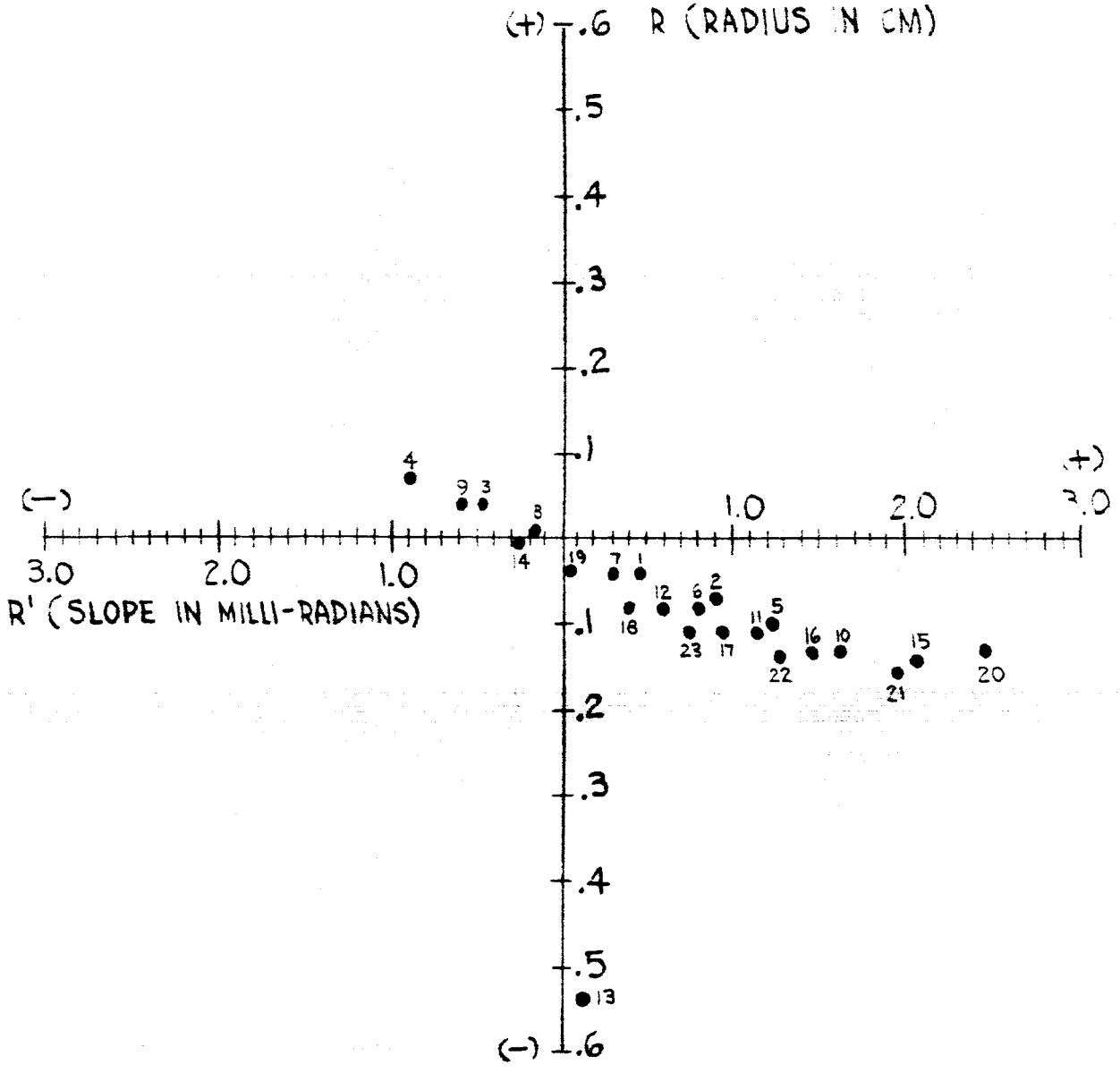

FIG. 10- INPUT EMITTANCE PROJECTED TO TARGET (4 MV)

I-647

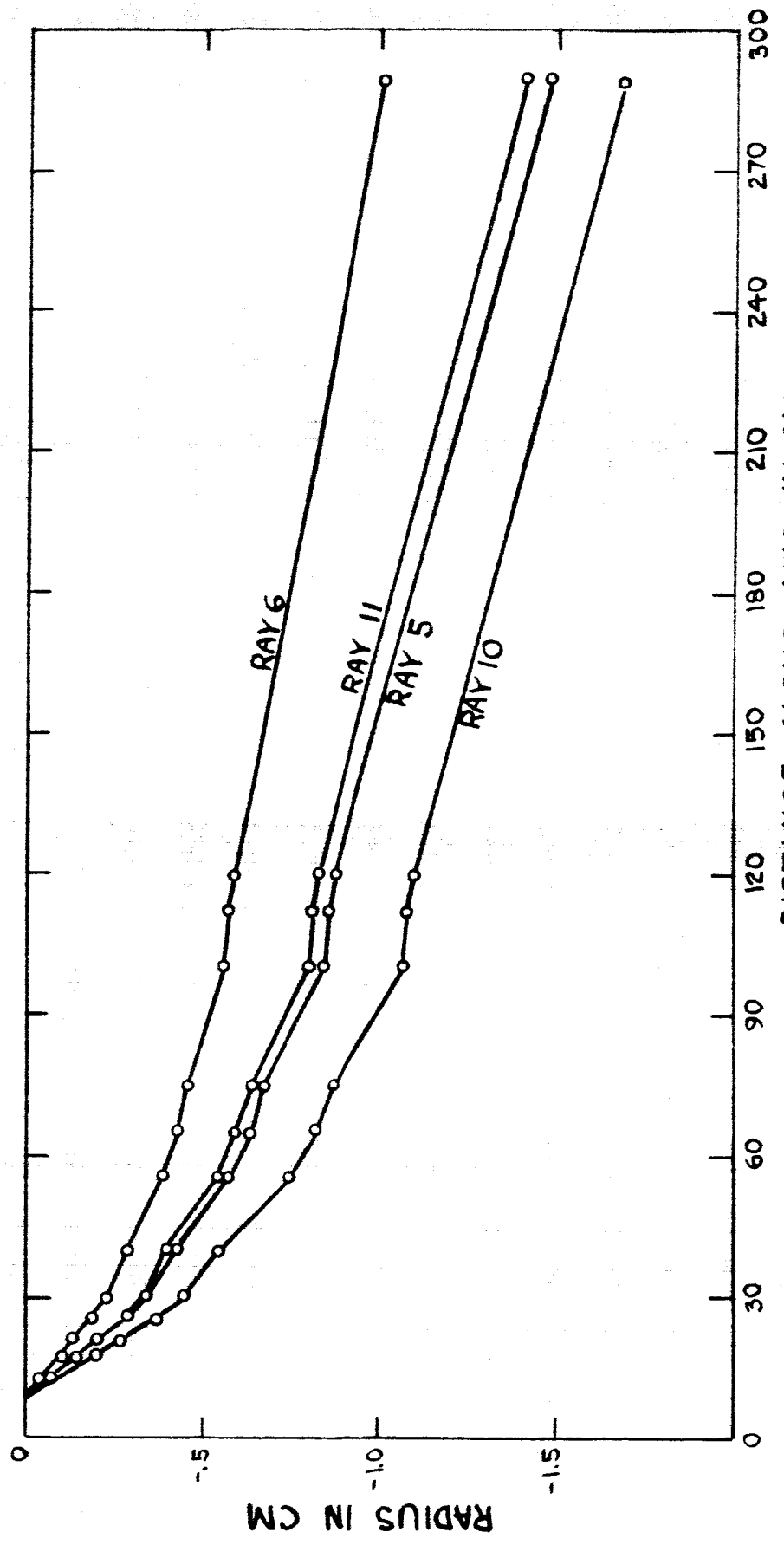

FIG. 11- RAYS THROUGH MICROMETEOROID ACCELERATOR
2 MV TOTAL POTENTIAL DROP

1-649

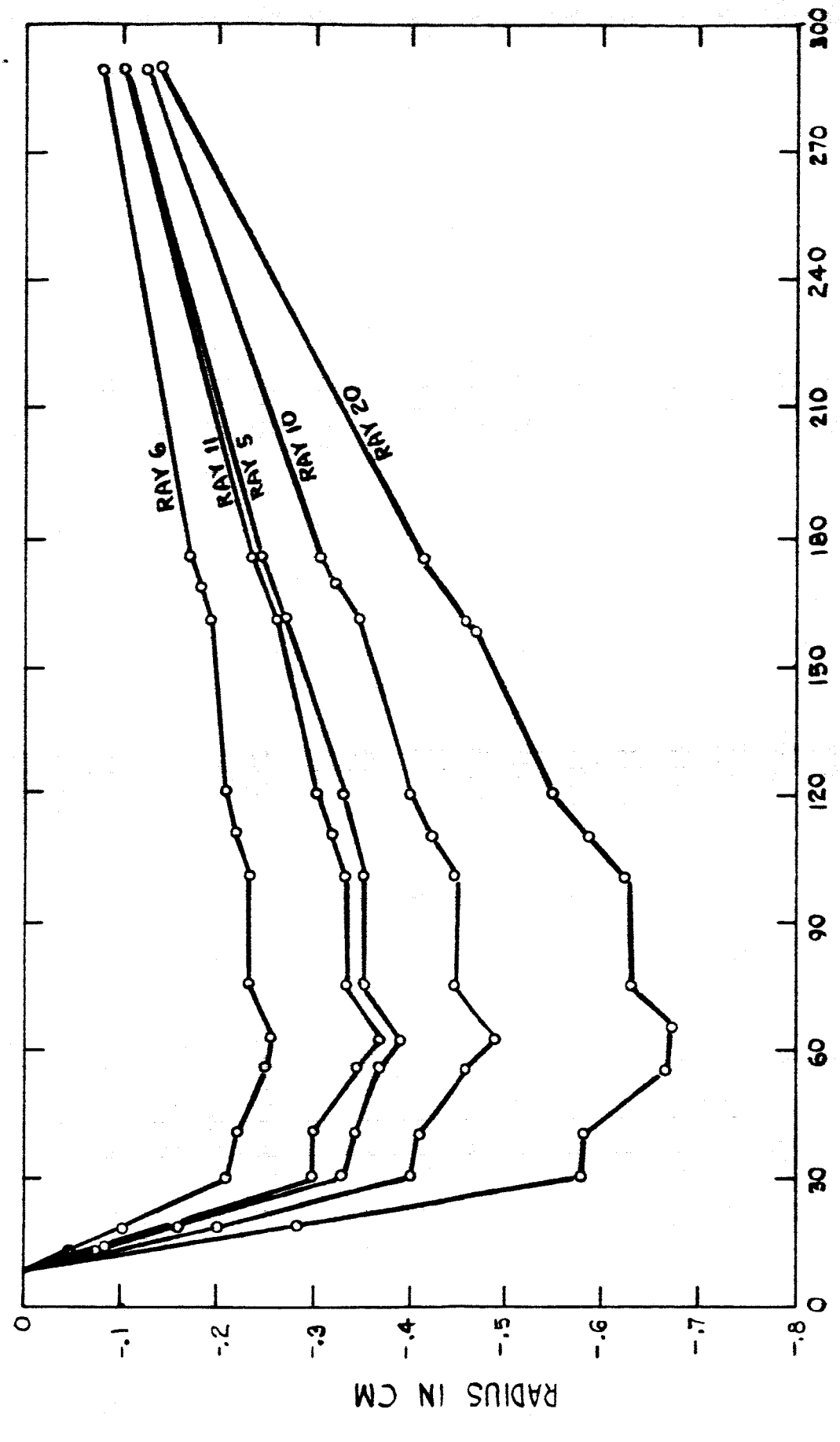

FIG. 12 - RAYS THROUGH MICROMETEOROID ACCELERATOR
4 MV TOTAL POTENTIAL DROP

Phase Focusing

The essence of phase focusing in an accelerator of the type proposed is that the drift tubes provide electrostatic shielding over a length long enough to cover timing uncertainties in the delay and switching circuits and position uncertainties due to variations in charge-to-mass ratio and stage voltage. Because the stage voltage is fixed, tube lengths required to cover position uncertainties are the same for all charge-to-mass ratios. This is not true of the timing uncertainties.

In discussing position uncertainties, it is convenient to define both a fast and a slow particle having the same nominal charge-to-mass ratio (ν). The fast particle, having speed U_f, has a charge-to-mass ratio of $1.01\ \nu$*, is expelled from the source with energy corresponding to 275 volts**, is pre-accelerated to 5005 volts and is accelerated at each stage through a potential difference 5% above nominal. The slow particle, having speed U_s, is expelled from the source with charge-to-mass ratio 0.98ν (1% initial uncertainty plus an immediate 1% loss) and energy corresponding to 225 volts, is pre-accelerated to 4995 volts, suffers a further charge loss of 9% to $0.89\ \nu$, and is accelerated at each stage through a potential difference 5% below nominal. The distance between the slow and fast particles at the moment when the fast particle is at shielded distance within the far end of a drift tube will be denoted by ΔS_{sf}. This is the principal position uncertainty.

The accelerator is assumed to be actuated at the beginning of the decaying portion of the detector signal which occurs over the last 0.25 cm of detector length (see detector specifications in Subsection 3.2.4). The

*Uncertainty in ν at the particle source is taken to be $\pm$ 1%.

**Source expulsion voltage is assumed to be 250 $\pm$ 25 volts.

detection uncertainty thus introduced may be as large as 0.25 cm and is amplified down the accelerator in proportion to the speed. At any stage, this uncertainty has magnitude ΔS_d given by

$$\Delta S_d = 0.25\, U_s/U_o = 0.1017 \sqrt{V_s}\ (\text{cm})$$

where U_o is the value of U_s at the detector and V_s is the total (nominal) potential drop in kilovolts up to and through the stage. The length of drift tube required for electrostatic shielding will be denoted by ΔS_{sh}. In Subsection 2.2, this was taken to be three tube radii. In Fig.13, the axial potential across an acceleration gap and through the end of a drift tube, as calculated on a computer, is given for both the 2.5 cm and 5 cm gaps. It is apparent that the assumed length provides shielding to better than one part in a thousand even if the tube positioning error of 0.25 cm is accounted for in this distance.

Time uncertainties arise both in the delay electronics and in the switching. If the delay is $T_s \pm \Delta T_d$ and the time required for switching is at most ΔT_s, then the drift tube length required is equal to $(2\Delta T_d + \Delta T_s)$ U_s. From the specifications of Subsection 3.2.4, the time ΔT_s is 1.9 μsec and ΔT_d is 2% of the full scale value of T_s (i.e., either 0.2 μsec or 2 μsec).

The total drift tube length can now be written as

$$S = \Delta S_{sf} + \Delta S_d + \Delta S_{sh} + (2\Delta T_d + \Delta T_s)\, U_s.$$

The lengths which have been specified earlier were determined by calculating ΔS_{sf} on the assumption of linear potential variation in the acceleration gaps with no fringing field. Once the lengths were chosen, exact calculations were made on the computer both for verification and to establish an accurate time

record for stage sequencing purposes. This was accomplished by tracing the paths of slow and fast particles through the accelerator as a function of time. The slow particles were started off axis since nonaxial rays are somewhat slower than axial rays. The results of these calculations are summarized in Table 1 wherein minimum required and actual drift tube lengths are compared for 4 MV total accelerating voltage. The length segments corresponding to timing uncertainties have been evaluated at the charge-to-mass ratios giving the largest values. The value of ΔT_s has been taken to be 0.9 μsec instead of 1.9 μsec in the expectation that improvements in switching speed will have been made by the time the accelerator may be modified for 4 MV operation. This value of switching time is in fact probably achievable even now. The fact that S exceeds the actual length for stage four by 0.62 cm is not troublesome since the shielding length of 3.75 cm is really 0.875 cm longer than is necessary, as is evident from Fig. 13. A similar comparison of required and actual drift tube lengths for 2 MV accelerating voltage is given in Table 2. Here the specified switching time of 1.9 μsec has been used.

Table 1. Comparison of Required and Actual Drift Tube Lengths for 4 MV Total Potential Drop (all lengths in cm)

Tube No.	ΔS_d	ΔS_{sh}	ΔS_{sf}	$(2\Delta T_d+\Delta T_s)U_s$	S	Actual Length
1	2.27	7.50	3.29	2.67	15.73	18.0
2	3.94	7.50	9.83	4.94	26.21	29.3
3	5.09	7.50	17.75	8.48	38.82	40.6
4	6.02	7.50	27.30	12.60	53.42	52.8

Table 2. Comparison of Required and Actual Drift Tube Lengths for 2 MV Total Potential Drop (all lengths in cm)

Tube No.	ΔS_d	ΔS_{sh}	ΔS_{sf}	$(2\Delta T + \Delta T_s)U_s$	S	Actual Length
1	2.27	7.50	3.24	4.74	17.75	18.0
2	3.22	7.50	8.51	6.69	25.92	29.3
3	3.94	7.50	15.45	8.44	35.33	40.6
4	4.54	7.50	24.13	12.80	48.97	52.8

Let T denote the time between actuation of the accelerator and the arrival of the slow particle at the shielded position in a drift tube. Then the appropriate delay time for the stage is

$$T_s = T + \Delta T_d.$$

Since the accelerator is a fixed voltage device, the time T is inversely proportional to the square root of the (nominal) charge-to-mass ratio or

$$T = t/\sqrt{\nu}\,.$$

A knowledge of the value of t for each stage is sufficient to enable the programming of the machine for any charge-to-mass ratio. The values of t derived from the computer calculations are presented in Table 3 for both 2 MV and 4 MV.

Table 3. Values of the Sequencing Parameter t (in units of μsec $[\text{coul/kg}]^{1/2}$)

Stage No.	t	
	2 MV	4 MV
1	415.1	415.6
2	643.6	633.4
3	898.4	839.7
4	1179.3	1056.5

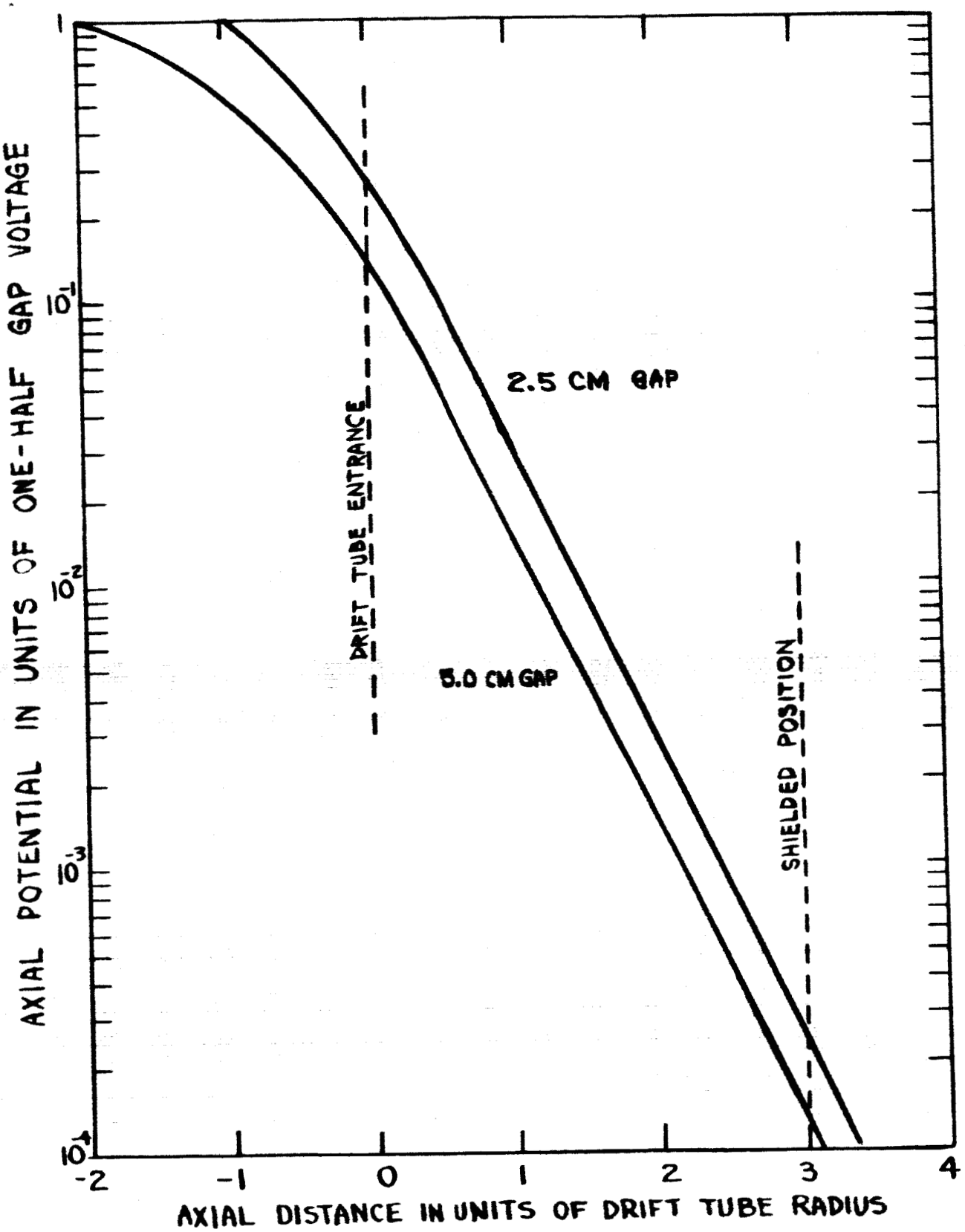

FIG. 13 - AXIAL POTENTIAL FROM CENTER OF ACCELERATION GAP TO SHIELDED POSITION IN DRIFT TUBE

1-651

3.3 ENVELOPE SYSTEM DESIGN

3.3.1 Tankage and Supporting Structures

The main vacuum vessel, including all port assemblies except flanges, is to be constructed of 304 stainless steel 3/8 in. thick. Flanges may be of other varieties of stainless steel and may be thicker. All flanges will be O-ring sealed. The ends of the vessel will be standard elliptical dished plates, I.D. = 4 ft, S.F. = 1 in. The cylindrical center section will be 4 ft i.d. by 40 in. long. The bottom of the cylindrical section and the top of the bottom end plate will flanged so as to form a bolted joint sealed with an O-ring. There will be a flanged 6 in. i.d. port opening in the center of each end plate and two diametrically opposed tandem pairs of 12 in. i.d. flanged openings in the center cylindrical section as indicated in Figs. 1 and 2. The center section will also be fitted with two 12 in. i.d. viewing ports as indicated in the figures. The top end plate will have a 12 in. i.d. right angle elbow faired into it, as shown in Fig. 2, to provide a pumping path. The elbow material should be 304 stainless steel 3/8 in. thick. This elbow will be fitted with an opening suitable for the mounting of an ionization type vacuum gauge. The exit port assembly in the bottom end plate will also provide mounting for an ionization type vacuum gauge. The main vacuum vessel should have openings suitable for supplying and venting liquid nitrogen and helium to the cryogenic pump. The pressure vessels will be constructed of steel. The cylindrical center section will have 3/8 in. wall thickness and will be approximately 16 in. i.d. by 22.5 in. long. The vessel wall thicknesses chosen (for both vacuum and pressure components) are deemed adequate to withstand the stresses due to pressure differentials resulting from evacuation or pressurization. The specification of 304 stainless steel in the vacuum components is again made because of its apparently superior high voltage breakdown characteristics. Since the estimated weight of the accelerator is just under 4000 lbs, each of the supporting stanchions and those parts of the supporting structure fastened to the main vacuum vessel must be capable of bearing at least 1000 lbs.

3.3.2 Vacuum Equipment

Diffusion Pump, Forepump and Baffle

For the purposes of these pumping system considerations, we shall assume that the injection device imposes no gas load upon the main pumps. This assumption is of course valid since the ARC injector possesses its own diffusion pumping system and cryopump and is separated from the main vacuum vessel by a relatively low conductance path; i.e., the degree of vacuum isolation is excellent. The prime load on the pumping system is therefore imposed by the rate of evolution of gases from the metallic and non-metallic surfaces of the chamber which, in turn, is dependent upon the duration of exposure of these surfaces to high vacuum. This aspect of vacuum engineering ultimately reduces to empirically based estimates as the precise nature of gas evolution as a function of time, material, surface condition, etc., is not known although various investigators have reported analyses which satisfy the widely diverging experimental findings in this field.[6-9]

As a result, the pumping system used in the accelerator will be based largely upon our laboratory experience with several systems of similar geometry and volume in which ultimate pressures in the 10^{-7}-10^{-8} torr regime have been accomplished under less ideal conditions than those involved in this instrument; i.e., normally larger condensible vapor loads or controlled gas throughputs are encountered.

The main vacuum system is fabricated from 304 stainless with standard dished stainless end plates of 120 cm internal diameter. The length of the main vessel is 100 cm leading to an exposed internal surface area of $\sim 6 \times 10^4$ cm^2. In addition, the isolation grid will increase this figure by $\sim$ 30% while the helium cryopump liquid nitrogen cooled shrouds and associated (2) heat shields together will possess exposed surface areas of $\sim 2.5 \times 10^4$ cm^2. As a result, the total exposed surface area of stainless will be

taken to be 10^5 cm^2. An initial outgassing rate of 10^{-9} torr-liter/sec cm^2 will be used for these surfaces; an acceptable compromise between the results of Blears and those reported from work at this facility.[10]

The second major contributor to system outgassing will be the exposed surfaces of the graded bushings which consist primarily of glass on the vacuum side and total 10^4 cm^2 for the four units. Using the data of Cartwright[8] for Pyrex at room temperature, an initial outgassing rate of 10^{-8} torr-liter/sec cm^2 will be assumed. The existence of other "real" leaks and back-diffusion loading from the diffusion pump itself will be ignored as leak rates as low as 10^{-9} atm c. c. /second may be diagnosed and corrected by helium leak detection techniques.

The initial gas loading of the system $Q = Q_{wall} + Q_{bushing}$

$= (10^{-4} + 10^{-4})$ torr-liter/sec.

Therefore, the pump speed required at 10^{-6} torr is 200 liters/second.

Experience has shown that well-trapped mercury pumped systems provide the most reliable performance for systems subjected to intense electric fields (conventional electrostatic accelerators, vacuum insulation test stands, etc) and as a result a 10 in. diameter (e.g., CVC type MHG-900) mercury pump will be used with a suitable high conductance freon cooled chevron baffle (e.g., CVC type BCR-101). This pump baffle system will be connected to the vessel head by a 90° cylindrical elbow of 12 in. inside diameter and arms of 20 in. length. Davis'[11] results give a conductance of 1560 liters/sec for air at NTP for such an L. The conductance of the suggested chevron baffle is 2600 liters/sec and the net conductance F, of the baffle-L system is $(1/F_B + 1/F_L)^{-1}$ = 1000 liters/second, a figure well above the 200 liters/second required by the initial outgassing load of the system. Thus, the calculated pumping speed S, where $1/S = 1/S_p + 1/F$,

will be 600 ℓ/sec where S_p is the rated speed of the pump in the 10^{-6} torr range. These characteristics are compatible with pumpdown times from roughing pressures (10^{-4} torr) to base pressures (10^{-7} torr) of only a few minutes, at which time the cryopumps can be brought into operation.

The forepressure tolerance of the primary diffusion pump is ~ 0.2 torr and its foreline shall exhaust into a two-inch mercury booster pump with a forepressure tolerance of 30 to 35 torr. This intermediate booster exhausts into a freon cooled mercury trap and then into a single stage rotary piston backing pump. The pump size must be chosen to provide a reasonable system roughing time. Assuming a crossover pressure (at which point the diffusion pump heaters are activated) of 30 torr, and a system volume of 1100 liters, a pump of the 6 to 8 liter/second class will provide a reasonable (10 minute) pumpdown time from atmospheric pressure; e.g., the Nash MD-674 (8 ℓ/sec).

A magnetically operated vacuum valve will be installed between the two-inch booster and the nine-inch diffusion pump for protection of the chamber in the event of a power failure. The diffusion pump heaters will also be interlocked with the primary coolant supply and the foreline valve will also be closed in the event of pump shutdown due to coolant loss. A 0 to 1 torr thermocouple gauge will be used to monitor forepressure between the freon cooled trap and protective valve in the foreline of the tandem mercury pumps. The scheme proposed will provide an effective barrier to contamination of the system with forepump water or atmospheric air. High temperature seals (Viton) will be used in the system where considered necessary (primarily on the diffusion pump face plate seals).

Cryopump

The pumping system described in the previous section will be capable of reducing the system pressure into the low 10^{-7} torr range after initial vacuum "soaking" or pumpdown of the chamber and bushings. Further reduction of chamber pressure will be accomplished with the use of a single cryopump. This unit will be made up of a peripheral double reflecting heat shield, a liquid nitrogen cooled shroud ($T < 100°K$) 100 cm in length and approximately 60 cm in width with a central helium cooled condenser ($T < 20°K$) with a total surface area of 3000 cm^2 ($\sim$ 30 cm x 50 cm).

The nitrogen cooled shroud will surround the planar 20°K panel and will be opaque on the side facing the chamber wall and of louvred or chevron geometry on the "pump" side such that free molecular flow is permitted. The nitrogen shroud, operating between 77°K and 100°K, will reduce the vapor pressure of CO_2 and all other gases except H, He and N_2 to $\lesssim 10^{-8}$ torr. Since the pumping speed of the outer array (considering sticking coefficients and capture probabilities in the system)[12] will be about 2 ℓ/sec/cm^2, a figure verified in our own nitrogen cryopump studies at IPC, a total speed of 20,000 ℓ/sec for condensibles will be provided by the nitrogen cooled portion of the pump itself. It is quite likely that the use of helium in the second pump element will not be resorted to in actual operation except where ultimate q/m ratios are desired ... its use will certainly be much less critical than it has found to be in the injector itself.

The fabrication of the cryopump will employ "standard panelcoil" where possible with vacuum insulated feedthroughs for both cryogenic supplies. The total thickness of the system must be minimized due to voltage insulation requirements. The thickness of the array from chevrons to outer reflective heat shields will be < 20 cm. Both the LN_2 and helium systems will be supplied with flow controllers such that wastage of cryogenic fluid is minimized. It is intended that self-pressurized dewars be employed as

primary reservoirs in each case and these shall be considered as an integral part of the accelerator. The flow control regulators for each will constitute a part of the vacuum system control panel at the operating console and the control of the cryopumps may be accomplished remotely from this point during operation of the accelerator.

3.3.3 Pressurization Equipment

The pressure vessels and feedthrough bushings must be insulated with mixtures of nitrogen, carbon dioxide, and sulfur hexafluoride gases. These will be supplied from commercial pressure bottles. Pigtails and valves will be furnished to connect these bottles to a standard gas manifold assembly as typically used by High Voltage Engineering Corporation for its accelerators. The assembly includes a 0-600 psi gauge, a 250 psi safety valve, a bleeder valve and an exit valve and a high pressure hose of about 15-foot length. Each pressure vessel and each bushing will be fitted with its own high pressure valve and connector for mating with the hose. A rotary mechanical vacuum pump with glass cold trap, dewar, 0-1 torr thermocouple gauge and hose will also be provided for vacuum drying the chambers prior to pressurizing. All of this equipment is of conventional design, readily available commercially.

Mechanisms for Increasing the Energy of Charged Particles*

Methods	Limitations and Problems	Geometrical Extrapolations
A - Constant Electric Field – constant electric charge on particle.	Particle orbit must begin and end at different potential levels. Present potential limit ~ 10^7 volts.	Typically linear machines.
B – Constant Electric Field – alternating charge on particle.	Particle charge is not easily reversed, particularly more than once.	
C – Alternating Electric Field – constant charge on particle.	Polarity reversal of E field must be synchronized with passage of particle through reduced-field (drift tube) region.	1. Simplest machines are linear. 2. Orbital machines are achieved by addition of a radial constraining force with magnetic or electric fields.
D – Traveling Electric Field – constant charge on particle.	Propagation velocity of maximum E region in field must match accelerating velocity of particle.	

*Acceleration of electric dipoles (asymmetrically charged particles) which have zero net charge are not considered here.

3.3.4 Radiation Shielding

Assumptions

The following calculation has been made to provide an intentionally conservative guidance in the selection of shielding materials for the ARC microparticle accelerator. In normal operation the drift tubes are held negative (-500 kV) and pulsed to ground during transit of the particle. As a result, the bremsstrahlung produced at the vessel walls by electrons desorbed from the drift tubes will constitute the prime radiation hazard. It is obvious that these radiation sources will be concentrated near the bushings themselves; i.e., the major emission will occur at the "field intensified" regions at the ends of the drift tubes and at the bushing terminations. However, since "variable" drift-tube polarity may be ultimately encountered in the accelerator, the radiation source is here considered to be a line bremsstrahlung source made up of the drift tubes and bushing terminations in the vacuum vessel. No radiation arising from the generators themselves is considered as the pressure vessel walls will suffice to suppress the weak radiation spectrum from each power supply. The "target" or anode is considered in all cases to be "thick" to the impinging electrons.

A cursory view of the accelerator geometry indicates that the "line-source" model used will provide conservative shield requirements since the shielding advantages due to "slant" incidence and localization in the actual "annular" source geometry are ignored. The assumption is therefore made that the annular source with effective source strength S_A per unit area and diameter d (120 cm) can be approximated by a line source with a strength per unit length of $S_L = \pi d\, S_A$.

Since the maximum bushing voltage is 500 keV, radiation spectra are considered on this basis while an electron drain current of 50 μA per unit is assumed as being the worst possible case for conditioning. Furthermore, a good deal of the conditioning current does not experience the total terminal potential but is rather handled in the graded structure which does not normally exceed 50 keV/section and hence, can generate no significant radiation (at least none that constitutes an external hazard). It is likely that conditioning currents may rise above this figure for brief periods, but the number taken as representative of "500 keV beam current" is probably conservative by a factor of five for normal conditions. The validity of these assumptions on "source strength" may be readily checked using scintillation spectrometer techniques during the conditioning of the first assembled 500 kV stage.

The assumed physical geometry of the system is shown below, in which the 150 cm line source of stainless (SS 304) is separated from the 1 cm (3/8 in.) thick stainless steel chamber wall by 60 cm.

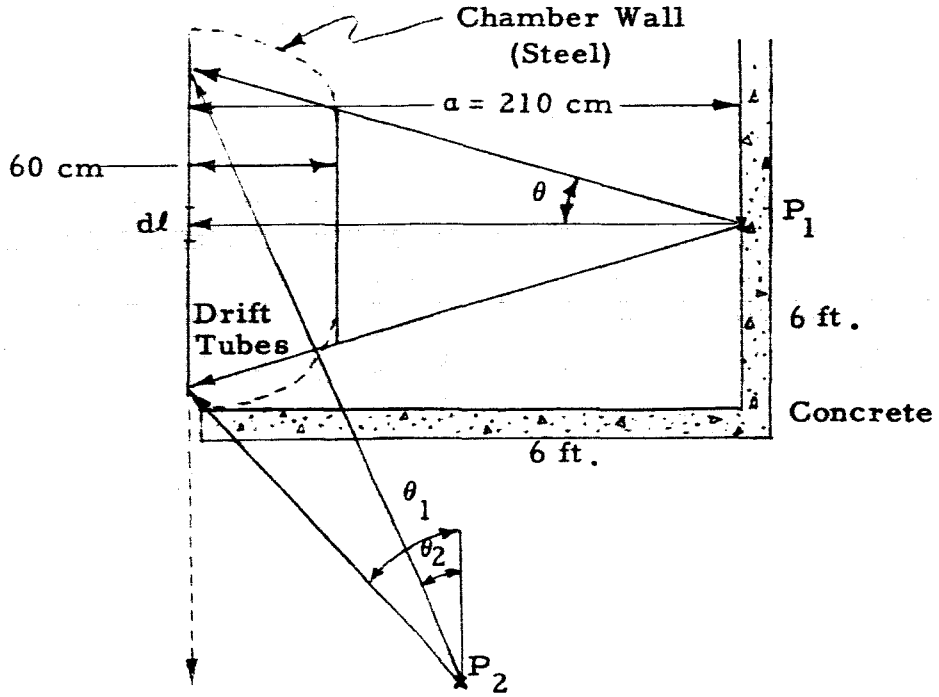

Fig. 14 Geometrical Model for Shielding Calculations

The minimum distance from the tank wall to the (assumed) concrete shield is 150 cm (5 ft) for all portions of the machine except the base. For the lower level dose considerations, the separation distances of tube-wall-shield are ignored and the dose level calculated at an assumed operator's station or point P_2, 1 meter off the beam axis and 1 meter below the machine floor-shield level. The "worst" case for the lateral shielding requirements is considered with the selection of point P_1 on the machine midplane.

The calculations will now be described for these two positions such that realistic estimates of floor and wall shielding requirements may be derived to maintain an environmental level of ≤ 2.5 mr/hr or the usual requirement of 100 mr or less for a 40-hr week. Steel with a density of 7.9 g/cm^3 and normal concrete with a density of 2.3 g/cm^3 are assumed in the calculations

Calculation

a. Side Wall at P_1

The bremsstrahlung spectrum may be calculated by the semi-empirical method of Greening[13] for the thick target case and such available data[14] for the 500 kV case will be used here. For these intermediate energies ($T_o = E_o/m_o c^2 \doteq 1$) only a few data[15] are available relating to angular distribution from thick targets and no analytical or empirical techniques are available. The angular distribution is much less peaked than at relativistic energies and the source is considered as isotropic for the purpose of the calculation. Using Buechner's[16] thick target data corrected for Z; i.e., Z = 26 for steel compared with 79 for Au, the case studied:

$$I \doteq (T_o)^{2.9} \doteq 3 \text{ r/min/ma at 1 meter for } T_o \approx 1.$$

For a current of 200 μA with stainless drift tubes:

$$D = 36 \text{ r/hr at 1 meter.}$$

Reducing this to flux, for an assumed mean spectral energy of 250 keV, the source strength:

$$S_o = 8 \times 10^{12}/\text{sec}$$

$$S_L = 5 \times 10^{10}/\text{sec/cm of the line source.}$$

If μ_1 and μ_2 are the linear absorption coefficients for steel and concrete respectively in cm^{-1} and t_1 and t_2 their respective shield thicknesses, the flux $d\phi$ at P_2 from a segment $d\ell$ of the source is:

$$d\ell = \frac{S_L \, d\ell}{4\pi (a \sec \theta)^2} \exp\left[-(\mu_1 t_1 + \mu_2 t_2) \sec \theta\right]$$

where

$$d\ell = a \sec^2 \theta \, d\theta, \qquad a = \text{the distance from } P_2 \text{ to mid-line}$$

Hence,

$$d\phi = \frac{S_L}{4\pi a} \exp(-\alpha \sec \theta) \, d\theta \qquad \text{and at } P_2$$

$$\phi = \frac{S_L}{2\pi a} \int_0^{19^\circ} \exp(-\alpha \sec \theta) \, d\theta$$

where

$$\alpha = \mu_1 t_1 + \mu_2 t_2.$$

Since

$\phi = 2 \times 10^{4}/cm^{2}/sec$ for the assumed tolerance level,

$$\int_{o}^{19^\circ} \exp(-\alpha \sec\theta)\, d\theta = 5 \times 10^{-4} \qquad \text{for which} \quad \alpha = 6.4 \text{ (see Ref. 17)}$$

and

$$\mu_2 t_2 = 6.4 - 1.0$$

where

$$\mu_1 = 1.01\ cm^{-1}$$

and

$$\mu_2 = 0.27\ cm^{-1}$$

$$\therefore\ t_2 = 20\ cm.$$

Since no consideration has been made of source thickness ("self" absorption) or of the additional shielding provided by the cryo-pump and external apparatus (supply pressure vessels, pumps), this shielding requirement for the worst position may be relaxed by at least 25%; i.e., a thickness of 15 cm is dictated.

b. **Lower Wall at P_2; i.e., Floor Shielding Requirements**

As before

$$d\phi = \frac{S_L\, d\ell}{4\pi(\alpha \csc\theta)} \exp(-\alpha \sec\theta)$$

where

$$d\ell = a \csc^2\theta\, d\theta$$

and

$$\phi = \frac{S_L}{4\pi a}\left[\int_o^{\theta_1} \exp(-\alpha \sec\theta)\, d\theta - \int_o^{\theta_1} \exp(-\alpha \sec\theta)\, d\theta\right]$$

$$= \frac{S_L}{4\pi a}\left[\int_o^{45^\circ} \exp(-\alpha \sec\theta)\, d\theta - \int_o^{22^\circ} \exp(-\alpha \sec\theta)\, d\theta\right]$$

$$S_L = 5 \times 10^{10}/\text{sec/cm}$$

and since

$$\phi = 2 \times 10^4/\text{cm}^2/\text{sec} \qquad \text{with} \qquad a = 202 \text{ cm}$$

we deduce

$$\int - \int = 1 \times 10^{-3} \quad \text{for which } \alpha = 5$$

$$\mu_2 t_2 = 4$$

$$\therefore\ t_2 = 15 \text{ cm.}$$

On the basis of these calculations, a primary concrete shield thickness of 15 cm is indicated for both the walls and floor of the accelerator cave. Further refinement of these calculations along with the shadow shield requirements for the exit tube port will be made at such time as the machine mounting geometry is firmly ascertained.

4. REFERENCES

1. Creed, F. C. and Collins, M. M. C., "The Measurement of Short Duration Impulse Voltages," I. E. E. E. Transactions, paper 63-39 (1963).

2. Wilkinson, K. J. R., "Some Developments in High-Power Modulators for Radar," J. I. E. E., 93 IIIA, 6, p. 1090, 1946.

3. Broadbent, T. E., Cooper, R., "Tripping a 1 MV Single Stage Impulse Generator," J. Sci. Instr., 38, 504, 1961.

4. Woolaver, L. B., "The Use of Triggered Spark Gaps as Crowbars," Proc. Seventh Symposium on Hydrogen Thyratrons and Modulators, p. 521, 1962.

5. Britton, R. B., Arnold, K. W., and Denholm, A. S., Rev. Sci. Instr. 34, 185, 1963.

6. Dayton, B. B., Vacuum Symposium Trans., 101, Pergamon Press, N. Y., 1959; also 8, 1961.

7. Hayashi, C., Vacuum Symposium Trans., 13, Pergamon Press, N. Y. 1957.

8. Dushman, S., Foundations of Vacuum Technique, Ch. 7, Wiley and Sons, N. Y., 1961.

9. Markley, F., Roman, R. and Vosecek, R., Trans. Eighth Vac. Symposium, Pergamon Press, N. Y., 1962.

10. Connor, R. J. et al, ibid, 1151.

11. Davis, D. H., J. Appl. Phys., 31, 1169, 1960.

12. Moore, R. W., Trans. Eighth Vac. Symposium, 426, 1, Pergamon Press, N. Y. 1962.

13. Greening, J. R., Br. Jour. Radiol. 24, 204, 1951; 27, 532, 1954.

14. Hine, G. J. and Brownell, G. L., "Radiation Dosimetry," Ch. XII, 539-541, Academic Press, Inc., N. Y., 1956.

15. Koch, H. W. and Motz, J. W., Rev. Mod. Phys., 31, 920, 1959.

16. Buechner, R., etal, Phys. Rev., 74, 1348, 1948.

17. Rockwell, T., "Reactor Shielding Design Manual," McGraw-Hill, pp. 385-392, N. Y., 1956.

UNCLASSIFIED

Contract NAS2-1873 April 1964

ERRATA

The following corrections are applicable to the Final Report entitled " A Preliminary Design Study of a Microparticle Accelerator" prepared for Ames Research Center, NASA, Moffett Field, California, under Contract NAS2-1873.

Page 3

Second paragraph, line 3 should read " method (D), the line integral of the field between source and target is.. "

Page 4

Second paragraph, line 11 should read " reverse polarity of) each joint or support as the particle passes through"

Page 6

Inadvertently omitted from report, please insert. 20 copies and vellum attached.

Page 29

First line should read " specification of 1 μsec is thought to be conservative in view of the pres-"

Page 39

Second paragraph, line 13 , word should be "denoted" not devoted.
Last line should read **Source expulsion voltage is assumed to be 250 ± 25 volts.

Page 48

Second paragraph, last line should read "it has been found to be....."

Page 52

Equation on last line should read: $I = 3(T_\bullet)^{2.9} \doteq 3$ r/min/ma at 1 meter.....

Page 53

Line 9, line 12 and line 14, should be P_1 instead of P_2.

Page 54

Paragraph b.....As before

$$d\phi = \frac{S_L d\ell}{4\pi\,(a \csc\theta)^2} \exp.....$$